



Understanding planktonic diatoms to inform site selection for shellfish offshore aquaculture systems

Carla S. Freitas^{a,*}, Priscila Goela^{a,b}, John Icely^{a,c}, Bruno D.D. Fragoso^{a,c}, Luciano de Oliveira Júnior^a, Sónia Cristina^a, Alice Newton^a

^a CIMA - Centre for Marine and Environmental Research/ARNET - Aquatic Research Network, FCT, Universidade do Algarve, Campus de Gambelas, 8005-139, Faro, Portugal

^b S2AQUAcoLAB, Olhão, Portugal

^c Sagremarisco Lda., Rua Ribeira do Poço, n.º26, 8650-426, Vila do Bispo, Portugal

ARTICLE INFO

Keywords:

Diatoms
Pseudo-nitzschia
 Portuguese coast
 Upwelling
 Bivalves
 Offshore aquaculture

ABSTRACT

Sustainable bivalve aquaculture offers a solution to rising food demand. This study aimed to help identify suitable offshore shellfish aquaculture sites in coastal upwelling regions. Here, planktonic diatom abundance, crucial for bivalve growth, is a key success factor. A successful bivalve production area was analysed to understand how diatom dynamics and upwelling influence a suitable location for shellfish offshore aquaculture. A diatom-based criterion for site selection is proposed. Surface water samples were collected over two years in southwest Iberia, near a major upwelling centre. Phytoplankton abundance and composition were assessed along with chlorophyll-a concentration and wind-stress upwelling indices. Episodes of high diatom concentrations were frequent and distributed throughout the year. Most diatom blooms were dominated by *Pseudo-nitzschia*, particularly the *delicatissima* group. Although this genus is potentially toxic, the levels of amnesic shellfish poisoning (ASP) toxin - the domoic acid (DA) in bivalves were mostly low or undetectable, even during periods of high *Pseudo-nitzschia* abundances. Conversely, the less abundant *Pseudo-nitzschia seriata* group presence often coincided with detectable DA in bivalves. These findings suggest that high *Pseudo-nitzschia* abundance does not hinder aquaculture and may even benefit it when the *delicatissima* group prevails in high numbers. Focusing on the *Pseudo-nitzschia seriata* group in predictive models may better predict DA levels for harvest closures, minimising economic losses and health risks. This is particularly true for locations where the *seriata* group is the one linked to DA production. Additionally, we identified oceanographic conditions coinciding with DA levels exceeding regulatory limit.

1. Introduction

Aquaculture plays an increasingly essential role in providing nutrient-rich, Blue Food, as highlighted by the *State of World Fisheries and Aquaculture report – Towards Blue Transformation* (FAO, 2022). Blue Food, which includes aquatic-derived protein sources rich in essential micronutrients and heart-healthy fatty acids, is crucial for meeting the rising global demand for nutritious food. Developing the potential of aquatic ecosystems offers a promising solution for sustainable, low-impact food in comparison to land-based animal protein production that poses significant environmental challenges (Suplicy, 2020). The expansion of aquaculture has become even more critical as capture fisheries face stagnation due to overexploitation. The FAO notes that 89

% of marine fish stocks are fully exploited or overfished, underscoring the need for aquaculture to meet future food demands while maintaining marine ecosystem health (FAO, 2024). Molluscs, particularly mussels, comprise a significant portion of aquaculture in the European Union (Avdelas et al., 2021). Currently, inshore sites nearing saturation are encouraging a shift towards offshore farming, which is seen as more environmentally sustainable, despite some localised effects demonstrated on water circulation (Galparsoro et al., 2020; Mascorda-Cabre et al., 2024). Offshore mussel farming, a non-fed aquaculture, is a sustainable practice that aligns with the Blue Transformation agenda by relying on naturally available resources. Mussel growth and production in these systems are heavily influenced by the availability and quality of phytoplankton, which directly affects growth and yield rates (Camacho

* Corresponding author.

E-mail address: clfreytas@ualg.pt (C.S. Freitas).

<https://doi.org/10.1016/j.marenvres.2025.107200>

Received 2 November 2024; Received in revised form 27 April 2025; Accepted 29 April 2025

Available online 1 May 2025

0141-1136/© 2025 The Authors. Published by Elsevier Ltd. This is an open access article under the CC BY-NC license (<http://creativecommons.org/licenses/by-nc/4.0/>).

et al., 1995). Therefore, careful monitoring of water quality and phytoplankton abundance is essential for assessing productivity when expanding offshore aquaculture operations.

Diatoms are a major component of marine phytoplankton, holding great ecological importance across all oceanic regions. They often dominate coastal waters, contributing up to 50 % of global marine primary productivity (Bach and Taucher, 2019) and are vital in offshore aquaculture areas, where they are known to support bivalve growth (Pernet et al., 2012). Diatoms are particularly beneficial for mussel growth (Pronker et al., 2008; Maloy et al., 2013) due to their high fatty acid content (Muñiz et al., 2019) and high biomass. Additionally, their predominant large cell size allows them to be retained by bivalves, as these organisms filter particles with more than 7 µm (Strohmeier et al., 2012). However, some diatom species can produce toxins or harm bivalves in other ways, leading to deleterious economic and public health consequences. Therefore, assessing the structure and dynamics of planktonic diatom communities is important for effective bivalve management in aquaculture.

The temporal dynamics of diatoms in the phytoplankton community are expressed by the temporal alterations in abundance, biomass, assemblages, and proportion to the other phytoplankton groups. These features are influenced by oceanographic parameters, which can vary with meteorology and hydrology. Coastal upwelling has been recognised as one of the main drivers of alterations in biomass, abundance, and structure of phytoplankton communities in Portuguese coastal waters (Moita, 2001). This is particularly strong in the Cape Saint Vincent (CSV) region (Alvarez et al., 2008; De Oliveira Júnior et al., 2024), which is located at the southernmost edge of the Portuguese branch of the Canary upwelling system, which is part of the Eastern Boundary Upwelling System, identified as a highly productive region of the ocean.

In the CSV region, coastal waters are often dominated by diatoms (Loureiro et al., 2005; Danchenko et al., 2019). Here, phytoplankton abundance has been linked to upwelling from various studies examining several groups of microplankton (Edwards et al., 2005; Loureiro et al., 2005; Goela et al., 2013, 2014; Danchenko et al., 2022), including groups associated with harmful algal blooms (HABs) (Lima et al., 2022). However, given alterations in ecosystems associated with climate change (CC), there is an increasing need for further research on this topic. Some authors suggest that CC may intensify coastal upwelling along the west Iberian coast during the 21st century (e.g. Sousa et al., 2017), potentially resulting in increased diatom abundance in the area. Conversely, other studies predict fewer and weaker upwelling events (Alvarez et al., 2008), which could lead to a reduction in diatom abundance. Regarding CC scenarios, the sea surface temperature (SST) along the Algarve coast, is expected to increase up to 1 °C under Representative Concentration Pathways (RCP) 4.5 and 2 °C under RCP 8.5 by the end of the century (Icely and Fragoso, 2023). In a study that explores the potential impacts of rising SST, changes on primary production and infection potential of *Marteilia refrigens* on mussel aquaculture the results are positive with reasonable projections of expansion of production and improved profitability (Icely and Fragoso, 2023).

In Portugal, toxin-producing diatoms have been monitored in bivalve mollusc harvesting areas by the Portuguese Institute for Sea and Atmosphere (IPMA), the national authority responsible for implementing European Union legislation to prevent acute poisoning in bivalve consumers (European Union, 2017). This comprises the official monitoring programme for toxic phytoplankton, known as SNMB – National Monitoring System for Bivalve Molluscs (IPMA, 2013). While crucial for ensuring food safety and minimising economic losses, the program focuses exclusively on potentially toxic species and does not encompass the entire diatom community.

The present study aims to assist bivalve farmers in identifying optimal conditions for new bivalve aquaculture facilities. To this end, a diatom-focused case study was conducted at a successful longline offshore bivalve aquaculture site (in the Sagres area, near CSV in the southwest of the Iberian Peninsula) known for its high mussel

productivity. By characterising the diatom community, similar conditions could be identified in other candidate locations for establishing comparable aquaculture systems. Thus, we sought to establish site suitability criteria for offshore bivalve aquaculture based on the phytoplanktonic diatom community. These could be applied to other areas of the globe with similar conditions. In this context, the following research questions concerning the diatom community were addressed:

1. Is the contribution of planktonic diatoms significant to productivity in the study area, standing out from the other phytoplankton groups?
2. Does upwelling positively influence diatom abundance and assemblages?
3. Can diatoms in the study area reach high densities (intense blooms) frequently throughout the year?
4. Are there concerns about toxin concentration originating from the diatom community?

Additionally, findings will contribute to valuable scientific insights for the sustainable development of aquaculture and enable comparisons with future scenarios to ascertain whether climate change is affecting diatoms.

2. Material and methods

2.1. Study area

The study is in the Sagres area, on the Atlantic coast off the Iberian Peninsula, in southwest Portugal (Fig. 1). The sampling took place at an offshore mussel farm located east of Sagres Harbour and approximately 1.3 km from the coastline with a depth of 20 m. West of Sagres, there is the CSV, approximately 5 km away. This region is directly affected by a southward upwelling jet that transports cold, nutrient-rich waters into the south coast of Portugal from upwelling that occur on the Portuguese west coast in response to the dominant northerly winds (Relvas and Barton, 2002; Sánchez and Relvas, 2003; Cravo et al., 2013). In addition, the CSV, being an upwelling centre because of windstress curl, experiences the most intense and frequent local upwelling along the southern coast of Portugal (De Oliveira Júnior et al., 2024). The upwelling season in the SW Iberian Peninsula is defined between March and October, with maximum intensity typically occurring in July and August (Fiuzza et al., 1982; Alvarez et al., 2008; Ramos et al., 2013). Along the south Portuguese coast, the upwelling intensity diminishes eastward and is generally less intense than that from the western coast due to weak western component of the wind (De Oliveira Júnior et al., 2024).

Despite the dominance of (weak) upwelling favourable conditions along the south coast, the shelf circulation flows alongshore in opposite directions (eastward and westward) throughout the year, with an average reversal interval of approximately four days (De Oliveira Júnior et al., 2022). The westward current, often called the coastal counter-current, is associated with the relaxation (or reversal) of the upwelling favourable conditions. During the warm months (May–October) these counter-currents are responsible for sharp temperature changes along the coast as they are carrying warm water from the east (Relvas and Barton, 2002; Garel et al., 2016; De Oliveira Júnior et al., 2022). These changes can reach up to 10 °C in the CSV region (Fragoso and Icely, 2009).

These coastal waters off the southwest Iberian Peninsula, where there are no river discharges and there are minimal inputs from terrestrial sources, rely primarily on upwelling as the main contributor to nutrient enrichment (Cravo et al., 2010). Furthermore, anthropogenic pressures are not significant, given the sparse resident population density and predominantly extensive agricultural activities.

The offshore bivalve aquaculture lease is located within the bivalve mollusc production area L7c1 (Litoral S. Vicente – Lagos) considered in the IPMA SNMB (<https://www.ipma.pt/pt/bivalves/zonas/>). Established in November 2010, this offshore aquaculture uses the longline

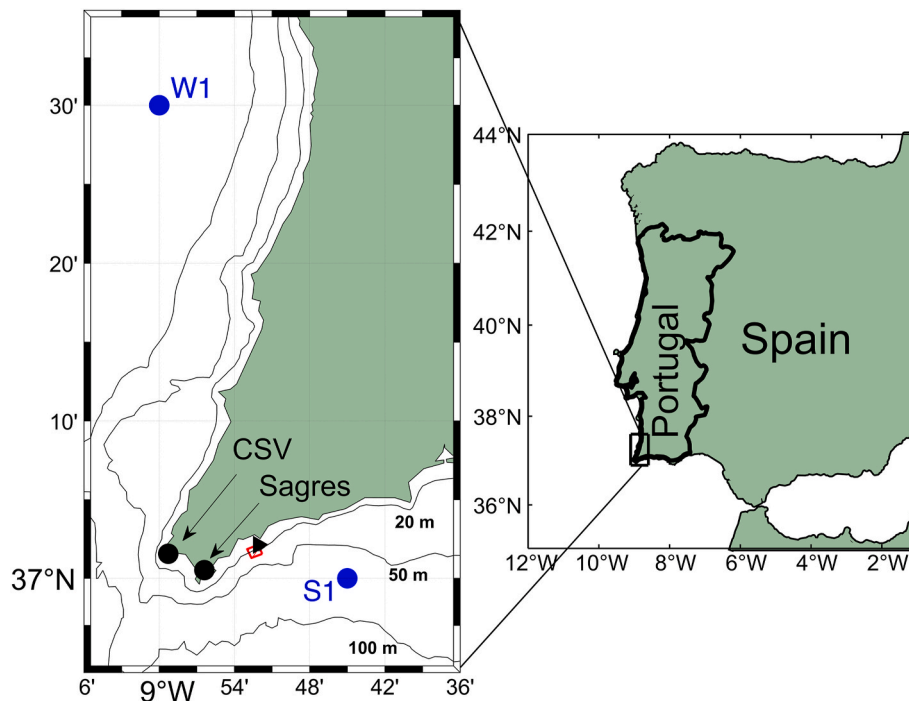


Fig 1. Geographic location of the sampling site off Sagres in the southwest coast of Portugal, situated on the Iberian Peninsula; the inset highlights the west coast of Algarve near Cape Saint Vincent (CSV) and Sagres. The red rectangle represents a bivalve offshore aquaculture. The black triangle represents the sampling site. The blue circles close to W1 and S1 indicate the geographic points W1 and S1 used to calculate the Upwelling Index (UI).

system for the cultivation of Mediterranean mussels (*Mytilus galloprovincialis*, Lamarck, 1819). This aquaculture has been the primary offshore mussel producer in the Algarve region, contributing approximately 1500 tons annually to the total mussel production in Algarve waters (<https://www.dgrm.pt/en/esta>). Notably, the farm has undergone two expansions, underscoring its successful operation and growth.

2.2. Sample collection

Surface water samples (0.5 m from the surface) were collected for quantitative analysis of phytoplankton (including diatoms) and chlorophyll *a* (Chla) concentration determination. For the former, standard volumes of 300–500 mL in tight-seal plastic bottles were immediately fixed with acidic Lugol's solution (1 %) and kept in the dark in a cool place till analysis. Water samples for Chla concentration determination were transported to the laboratory in opaque Nalgene® 10 L carboys. Samples were collected weekly, with some fortnightly collections from July 2018 to November 2020. The phytoplankton analysis included a total of 60 samples, 46 of which coincided with specific dates used for determining Chla concentration.

2.3. Upwelling index

Upwelling (downwelling) favourable conditions were assessed through the widely used upwelling index (UI) proposed by Bakun (1973) using hourly ERA5 wind speed and direction (at 10 m) time series (Hersbach et al., 2023). Wind data was filtered using a Butterworth filter of 40h to remove high-frequency oscillations.

UI quantifies the integrated transport of water perpendicular to the coast, driven by the wind component parallel to the coast. The location of the sampling area although located in the south coast it is affected by the water circulation dynamics from west coast and south coast, therefore, UI was estimated in two geographic points to capture upwelling/downwelling events from various wind directions: W1, located on the west coast (37.5°N; 9°W), and S1, on the south coast (37°N; 8.75° W) (Fig. 1). UI (units of $m^2 \cdot s^{-1}$) was computed for the W1 and S1 locations,

using MATLAB® following Bakun (1973) and Cropper et al. (2014) according to the following equation:

$$Q_x = \frac{\tau_y}{\rho f} \text{ and } Q_y = -\frac{\tau_x}{\rho f} \quad \text{Eq. 1}$$

Where f is the Coriolis parameter and $\rho = 1025 \text{ kg m}^{-3}$. Q_x and Q_y represents the zonal and meridional integrated transport as a function of the eastward τ_x and northward τ_y surface wind stress, respectively.

Since upwelling (downwelling) favourable conditions result from the northern component of the wind on the Portuguese west coast, and from the western component in the south coast, UI represents Q_x and Q_y at the W1 and S1 locations, respectively (with negative values indicating upwelling favourable conditions).

2.4. Chlorophyll-*a* concentration analysis

Chla concentrations were estimated following Parsons et al. (1984) under the Green Aquaculture Intensification in Europe (GAIN) European project (Icelly et al., 2022). Samples were homogenised and three replicates of 1.5 L were filtered through 47 mm Whatman® GF/F filters (0.7 μm pore size), which were preserved at -18°C until further analysis. For extraction, each filter was grounded with a glass rod into a 15 mL centrifuge tube with 10 mL of acetone 90 %, and the tube was agitated using a vortex. After 24–48 h in the freezer, the tubes were centrifuged (*P Selecta Centro 8-BL*) for 5 min at 3500 rpm. The supernatant was placed into a 1 cm path quartz cuvette and analysed using a Shimadzu UV-2401 spectrophotometer. Absorbances were measured at 664 nm and 750 nm wavelengths before and after acidification with 20 μl of 10 % HCl. Lorenzen's spectrophotometric equation (Lorenzen, 1967) was used for the calculation of Chla concentration.

2.5. Phytoplankton/diatom abundance and community composition

The enumeration and taxonomic identification of phytoplankton, including diatom cells, were conducted using a Zeiss® Axio Observer A1 inverted microscope with phase contrast, equipped with a digital camera

connected to a computer. The methodology followed the Utermöhl technique (Utermöhl, 1958) and adhered to European standards (CEN, 2011; CEN, 2006). Subsamples of 50 mL obtained after homogenisation were allowed to settle for 24 h. Microplankton were then counted across the entire chamber bottom at 100x magnification (400x magnification was used for identification when necessary). Nanoplankton and the most abundant species were counted in 25–40 fields at 400x magnification with a minimum count of 300 cells. This category includes a cell-size group of unidentified cells with a diameter of 2–10 µm - nanoplankton <10 µm. Picoplankton (cells under two µm in size) were not included in the enumeration. The calculation of cell density, indicated as abundance, followed European Quality Standards (CEN, 2006). The detection limit (DL) for counted microplankton cells was set at 20 cells.L⁻¹, applicable for diatoms and other phytoplankton groups larger than 20 µm. With the method adopted in this study, there is inherent uncertainty in distinguishing between live and dead diatom cells, particularly when reserve lipids and vacuoles are smaller than average. Because of uncertainty of the method in distinguishing between live and dead diatom cells, a precautionary principle was applied, and cells were counted in doubtful cases. The identification employed the currently accepted taxonomic names from AlgaeBase database (Guiry and Guiry, 2024).

2.6. Abundant, dominant and frequent species/taxa

On each sampling day, the abundance (cells.L⁻¹) was calculated for every species (or genus) present. Abundant and dominant species were identified based on the criteria established by Lobo and Leighton (1986). According to these criteria, species were considered abundant if their numerical occurrence exceeded the average value of the total number of individuals of different species in the sample. Dominant species were those with a density greater than 50 % of the total sample density. Additionally, the relative frequency was determined for each identified species, representing the occurrence frequency relative to the total number of sampling days. Taxa (species/genus) were considered frequent if their relative frequency surpassed the 75th percentile of the relative frequency of all species observed throughout the study, indicating their presence in more than 31.3 % of the sample days.

2.7. Bloom frequency and classification criteria

A phytoplankton bloom is typically characterised by an abnormally high cell count relative to the system's baseline, although there is no universally agreed-upon definition. In this study, the criterion chosen to define bloom conditions, from the diatoms' perspective, was the 75th percentile of diatom abundance, which equated to 650×10^3 cells.L⁻¹. Any sampling date with diatom abundance exceeding this threshold was classified as in bloom condition. Additionally, an exception was made for the sampling date 15.10.2019, where the recorded abundance slightly fell below this threshold (627×10^3 cells.L⁻¹). Despite this fact, a bloom condition was still considered due to its significant deviation from other values. Other bloom conditions were estimated for phytoplankton, using Chla as a proxy for phytoplankton biomass (Boyce et al., 2010). This was on sampling dates when Chla concentration data were available with diatom counts. The classification criterion was based on the 75th percentile of this dataset, with samples above the threshold ($2.25 \mu\text{g.L}^{-1}$) considered to be in bloom condition. The frequency of bloom events was assessed both in absolute numbers and as a ratio, expressed as the percentage of blooms relative to the number of samples during the period in question.

2.8. Toxic diatom events analysis

Some diatom taxa can produce toxins. Within the study area, frequent HABs are attributed to *Pseudo-nitzschia* H. Peragallo, 1900. Twenty-two species of this genus have been identified on the Portuguese coast (DGRM, 2020). According to Monteiro et al. (2024), this genus is

the sole genus responsible for Amnesic Shellfish Poisoning (ASP) HAB impacts in Portugal, which are registered in the Harmful Algal Event Database (HAEDAT) (IOC-UNESCO, 2022). Those occurrences are reported to this database when they trigger management actions, result in negative economic impacts, or produce ecological consequences (Hallegraeff et al., 2021). The pennate diatom genus *Pseudo-nitzschia* is globally distributed. Currently, it includes at least 62 species (WoRMS, 2024), 29 of which can produce the neurotoxin domoic acid (DA), responsible for ASP (Lundholm et al., 2009). Monitoring programmes often tailor *Pseudo-nitzschia* spp. cell abundance thresholds to anticipate ASP events, considering national specifics. Based on valve width, *Pseudo-nitzschia* species are classified into *seriata* (>3 µm) and *delicatissima* (<3 µm) groups (Hasle, 1965; Hasle and Syvertsen, 1997), both containing toxin-producing and non-toxic species.

Two approaches were employed to analyse toxic diatom events. The first of these approaches employed IPMA SNMB thresholds and its public online data (IPMA, 2022) the second utilised HAEDAT (IOC-UNESCO, 2022).

Firstly, we compared the abundance of ASP causative species in our dataset with the IPMA SNMB corresponding alert level. In cases of exceedance, these data were compared with their temporally corresponding records in the IPMA public database for the same area (IPMA, 2022). Subsequently, exceedances of IPMA's reference warning and closure thresholds (for assessing the risk of toxin-producing phytoplankton species levels in water) for the cell abundances of *Pseudo-nitzschia* subgroups (*delicatissima* and *seriata*) were identified. Additionally, bivalve domoic acid (DA) data from the IPMA database were assessed for these dates within the study area. Furthermore, bivalve DA concentration data from the IPMA SNMB public database (IPMA, 2022) for the study area and period were compared with regulatory limits (IPMA, 2022) to detect exceedances.

On the second approach, information from the HAEDAT database was primarily used to investigate ASP-related events. Concurrently, we compared the frequency of these events in our sampling area in Portugal (2018–2020) with those of other shellfish poisoning syndromes; Paralytic Shellfish Poisoning (PSP) and Diarrhetic Shellfish Poisoning (DSP).

2.9. Statistical analysis

Prior to characterising variable diatom abundance, a preliminary statistical descriptive analysis was conducted across the entire study period. A boxplot analysis was employed to identify potential outliers within this quantitative variable. If outliers were detected, descriptive statistical measures such as the median, quartiles, and interquartile range (IQR) were calculated. In the absence of outliers, the mean and standard deviation were determined.

Because the Kolmogorov-Smirnov test showed the non-normality of the data, the hypothesis of a correlation between Chla ($\mu\text{g.L}^{-1}$) and diatom abundance (cells.L⁻¹) was tested, using Spearman's rank test. A significance level of 5 % was adopted. The suitability of the chosen threshold for bloom in diatom abundance was evaluated by testing for significant differences between samples in bloom and non-bloom conditions using the Kruskal-Wallis test, with a significance level (α) of 5 %. The seasonality of diatom abundance was evaluated using the entire dataset of diatom abundance samples. A Kolmogorov-Smirnov test was initially conducted to evaluate dataset normality. As the results showed a non-normal distribution, the Kruskal-Wallis test was subsequently employed, with a significance level (α) of 5 %. Results were considered significant for the cases in which p was < α .

Statistical analysis was performed using IBM® SPSS® Statistics for Mac® version 28.0.1.1. Microsoft®Excel for Mac version 16.65 was used as a complementary tool for descriptive statistical analysis and graphics.

3. Results

3.1. Total abundance and temporal distribution of diatoms related to other microplankton groups and Chla

While unidentified nanoplankton cells $<10\ \mu\text{m}$ were numerically dominant, diatoms constituted the second most abundant phytoplankton group (Fig. 2a). Despite nanoplankton's numerical dominance, their average contribution to total phytoplankton abundance varied significantly, with ratios of 77 % during non-bloom conditions and 56 % during bloom conditions (defined by Chla concentration). This analysis considered sampling days where both Chla and phytoplankton counts were available. Notably, no significant correlation was found between Chla concentration, and nanoplankton abundance (Spearman's $\rho = 0.112$; $p = 0.457$). Conversely, diatom abundance exhibited a strong positive correlation with Chla concentration (Spearman's $\rho = 0.572$, $p < 0.001$), as defined by Cohen (1992), and demonstrated a clear

influence on Chla levels (Fig. 2b). This correlation indicates that diatom variability explained 32.7 % of the Chla variance on days with complete data, with an even stronger correlation observed during summer (Spearman's $\rho = 0.710$, $p = 0.004$).

Occasional discrepancies between Chla concentration and diatom abundance were observed (Fig. 2a and b). On 24.07.2019, the increase on Chla was primarily attributed to a high abundance of the dinoflagellate *Lingulaulax polyedra*. Conversely, a period of low Chla and concurrent low diatom abundance (30.08.2019) coincided with an exceptionally high abundance of nanoplankton $<10\ \mu\text{m}$ (92 % of total abundance), significantly exceeding their average contribution (73 %).

Diatom abundance ($\text{cells}\cdot\text{L}^{-1}$) exhibited significant variability throughout the study period, with outliers noted (Table A1 in Supplementary material) and a median value of $123 \times 10^3\ \text{cells}\cdot\text{L}^{-1}$. Diatom abundance ranged up to a maximum of $3000 \times 10^3\ \text{cells}\cdot\text{L}^{-1}$ on 30.09.2020 (Fig. 2b; Table A1 in Supplementary Material). The dataset revealed that 25 % of diatom abundance values exceeded $650 \times 10^3\ \text{cells}$

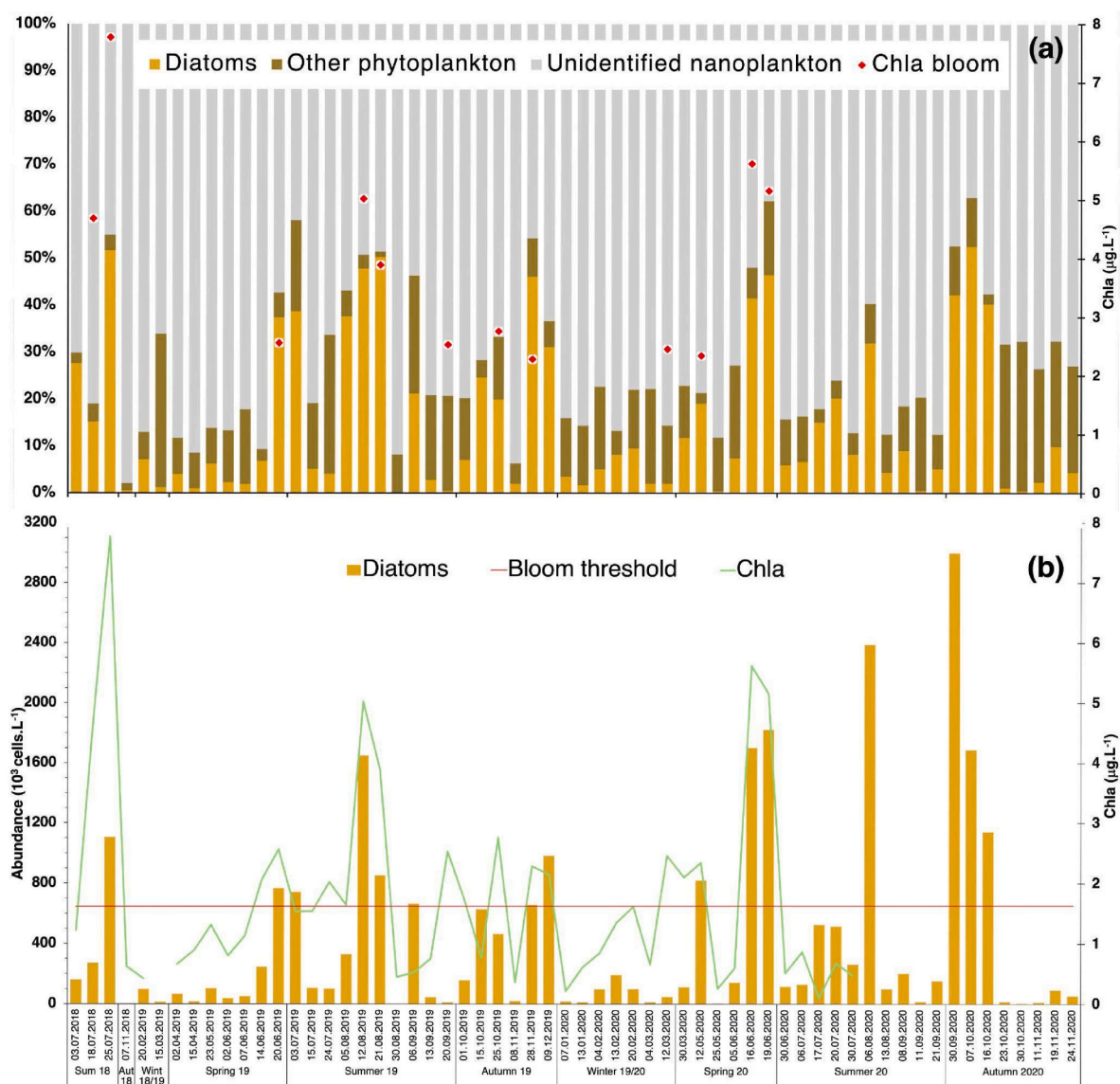


Fig. 2. (a) Temporal distribution of phytoplankton groups by relative abundance: diatoms (brown bars) unidentified nanoplankton $<10\ \mu\text{m}$ * (grey bars), and other phytoplankton** (olive green bars). Red dots represent Chla bloom conditions. (b) Temporal distribution of diatom abundance ($10^3\ \text{cells}\cdot\text{L}^{-1}$) and Chla concentration ($\mu\text{g}\cdot\text{L}^{-1}$) (green line), with the red line indicating the diatom bloom threshold ($650 \times 10^3\ \text{cells}\cdot\text{L}^{-1}$). * Unidentified nanoplankton $<10\ \mu\text{m}$ includes phytoplankton cells in the 2–10 μm size class that were difficult to identify due to their small size. **Other phytoplankton refers to the remaining phytoplankton, expressed as a percentage of the total phytoplankton cell count over the study period. (For interpretation of the references to colour in this figure legend, the reader is referred to the Web version of this article.)

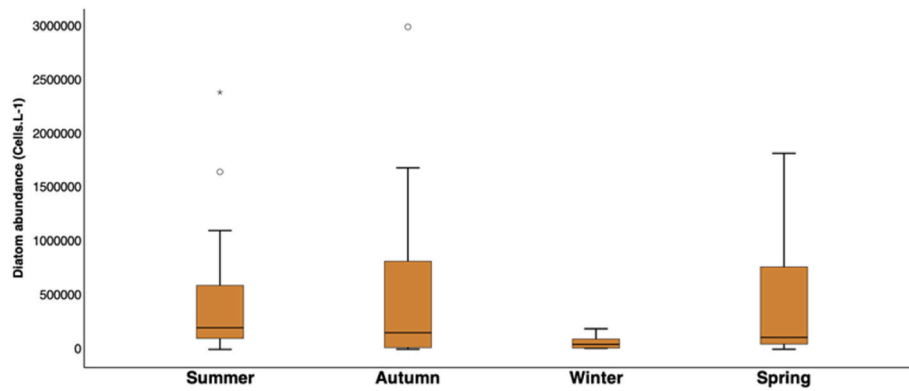


Fig. 3. Boxplot of diatom abundance (cells.L⁻¹) grouped by seasons (spring, summer, autumn, winter) during the study period.

L⁻¹, indicative of bloom conditions, while 25 % fell below 39×10^3 cells.L⁻¹, resulting in a substantial IQR of 611×10^3 cells.L⁻¹. This pronounced variability underscores the dynamic nature of diatom populations in the region, highlighting their potential for significant fluctuations in abundance.

While graphical representations suggested seasonal variations in diatom abundance (Fig. 3), statistical analysis revealed no significant differences in their overall distribution across seasons (Kruskal-Wallis test $p = 0.101 > \alpha = 0.05$; Kolmogorov-Smirnov = 0.266; $p < 0.001$). Despite quite similar median values (Fig. 3), the IQR varied, with spring and summer IQRs representing 89 % and 60 % of the autumn IQR, respectively. Winter exhibited a markedly lower IQR, only 10 % of autumn's, and a lower median of 47,974 cells L⁻¹, without observed extreme values or outliers (Table A1 in Supplementary Material; Fig. 3). Consequently, the spring-summer-autumn period demonstrated significantly higher diatom productivity compared to winter (Kruskal-Wallis test $H = 5.717$; $p = 0.017 < 0.05$).

Autumn 2019 and spring 2020 exhibited the highest bloom frequency, with 50 % of samples meeting bloom criteria (Fig. A1 in Supplementary Material). Overall, autumn showed the highest proportion of bloom events (40 %), followed by spring (31 %) and summer (26 %). Consequently, diatom productivity was significantly higher during spring, summer, and autumn compared to winter.

It is important to note that the lower number of winter samples may underrepresent winter conditions.

3.2. Diatom community structure

Throughout this study, a total of 74 diatom species spanning 43 genera (including unidentified species) were registered (Table A2 in Supplementary Material).

Pseudo-nitzschia spp. emerged as the most prevalent diatom taxon throughout the study period (Table 1) demonstrating the highest frequency, abundance, and dominance. Within this genus, the *Pseudo-*

Table 1

List of diatom taxa that were abundant on at least one sampling day, the percentage of sampling days in which they were abundant and dominant, their relative frequency of occurrence and identification of frequent taxa, listed from the most to the least frequent (in superscript).

Abundant species or taxa	Percentage of sampling days in which the taxa was abundant (%)	Percentage of sampling days in which the taxa was dominant (%)	Relative frequency of occurrence (%)
<i>Pseudo-nitzschia</i> spp.	58.3	16.7	95 ¹
<i>Leptocylindrus danicus</i>	48.3	13.3	76.7 ³
<i>Cylindrotheca closterium</i>	33.3	3.3	81.7 ²
<i>Chaetoceros</i> spp.	26.7	3.3	60 ⁷
<i>Guinardia delicatula</i>	20.0	–	68.3 ⁵
<i>Thalassiosira</i> sp.	18.3	3.3	43.3 ¹¹
Pennate diatoms unidentified	16.7	1.7	65 ⁶
Centric diatoms unidentified	15.0	–	36.7 ¹⁵
<i>Detonula pumila</i>	11.7	–	45 ⁹
<i>Leptocylindrus minimus</i>	10.0	–	21.7
<i>Bacteriastrum</i> sp.	8.3	–	3.3 ¹⁷
<i>Proboscia alata</i>	8.3	–	75 ⁴
<i>Skeletonema</i> sp.	8.3	–	3.3
<i>Dactyliosolen phuketensis</i>	6.7	–	26.7
<i>Guinardia striata</i>	6.7	–	38.3 ¹³
<i>Nitzschia</i> sp.	6.7	–	40 ¹²
<i>Eucampia cornuta</i>	5.0	1.7	30
<i>Bacillaria</i> sp.	1.7	–	3.3
<i>Cerataulina</i> sp.	1.7	–	5
<i>Chaetoceros peruvianus</i>	1.7	–	15
<i>Chaetoceros socialis</i>	1.7	–	1.7
<i>Cocconeis</i> sp.	1.7	–	1.7
<i>Amphiprora</i> sp.	1.7	–	6.7
<i>Guinardia</i> spp.	1.7	–	5
<i>Hemiaulus chinensis</i>	1.7	–	6.7
<i>Hemiaulus</i> sp.	1.7	–	5
<i>Lauderia annulata</i>	1.7	–	31.7 ¹⁹
<i>Meuniera membranacea</i>	1.7	–	20
<i>Sundstroemia setigera</i>	1.7	–	30
<i>Skeletonema</i> cf. <i>costatum</i>	1.7	1.7	3.3

nitzschia delicatissima group was observed in 87 % of sampling dates exceeding the 80 % occurrence of the *Pseudo-nitzschia seriata* group. *Leptocylindrus danicus* was the second most abundant and dominant taxon and was also highly frequent.

A general trend was observed where frequently occurring species also tended to be more abundant. This was supported by a moderate to strong positive correlation between the percentage of sampling days in which a species was abundant and its percentage of occurrence (Spearman's $\rho = 0.560$; $p < 0.001$). For instance, *Chaetoceros* spp. and *Cylindrotheca closterium* were highly frequent and abundant for a great number of sampling dates. However, these taxa were dominant in only two samples. Conversely, *Skeletonema cf. costatum*, occurred in only two samples and was only abundant and dominant once.

3.2.1. Temporal distribution of abundance for dominant species during the study

Pseudo-nitzschia spp. was the taxon that reached the highest abundance in 2019 (Fig. 4a). *Thalassiosira* spp. exhibited two significant abundance peaks, at the end of autumn, on the only sampling dates,

during the study, when this taxon was dominant (Table 1). However, no samples were available for the corresponding dates in 2018 and 2020. Another significant species in 2019 was *Leptocylindrus danicus*, which exhibited several peaks, mainly in spring and summer, but also in autumn. *Chaetoceros* spp. abundances exceeding $100 \times 10^3 \text{ cells.L}^{-1}$ were nearly absent in 2019, occurring only once (Fig. 4a).

In 2020, *Pseudo-nitzschia* spp. reached a markedly higher abundance than other diatom species (almost double that observed in 2019). These maxima occurred in the same month (August) in both years (Fig. 4a and b). The second-highest abundance in 2020 was recorded for *Skeletonema cf. costatum*, coinciding with the highest total diatom abundance observed in the study (Fig. 2b and 4b). *Pseudo-nitzschia* spp., *Leptocylindrus danicus* and *Chaetoceros* spp. exhibited a similar number of peaks exceeding $100 \times 10^3 \text{ cells.L}^{-1}$ in that year. However, *Chaetoceros* spp. peaks were restricted to spring and autumn, whilst *Leptocylindrus danicus* and *Pseudo-nitzschia* spp. peaked in spring, summer and autumn.

Leptocylindrus danicus, exhibited a similar number of peaks in both 2019 and 2020. The remaining species indicated in Fig. 4 were dominant only in samples with low total diatom abundance.

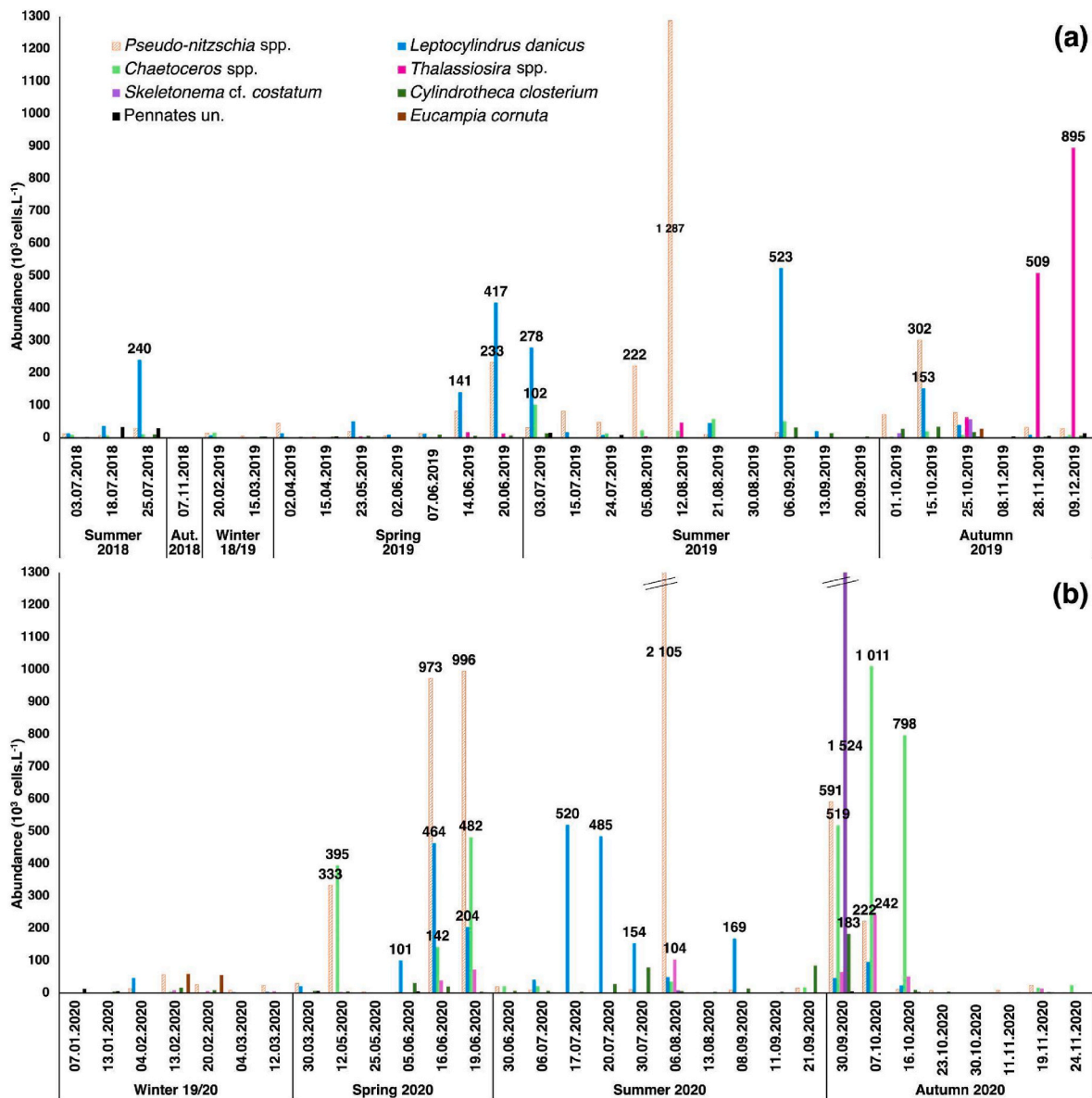


Fig. 4. Temporal distribution of the abundance of dominant diatom taxa during (a) 2018 and 2019 and (b) during 2020. Abundances above $100 \times 10^3 \text{ cells.L}^{-1}$ are identified with a label of abundance numbers.

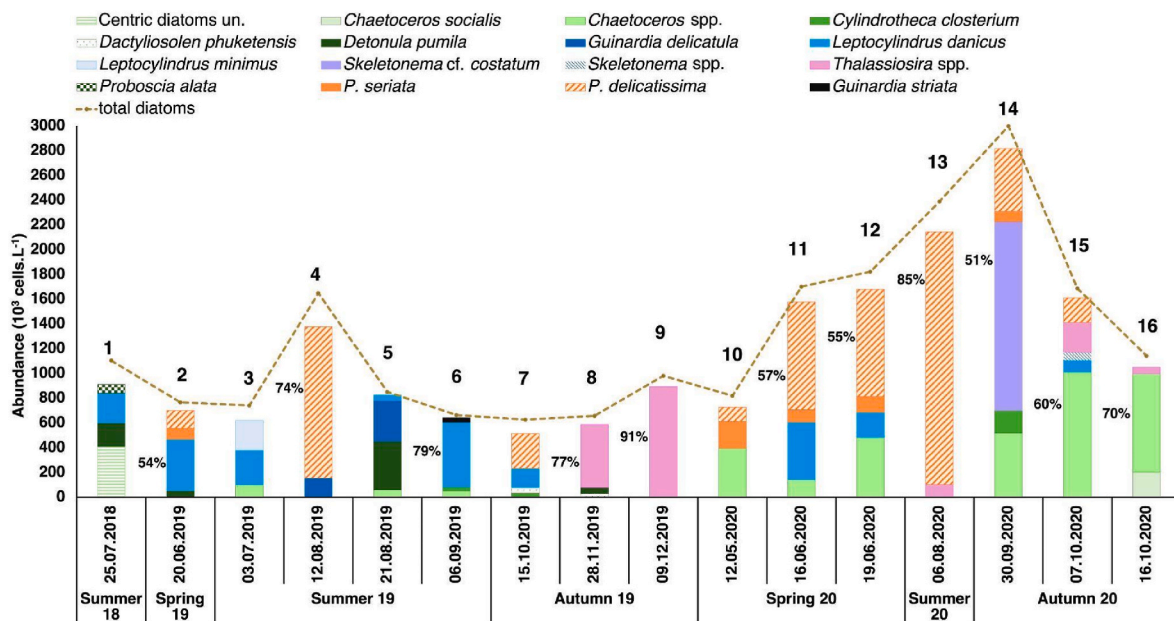


Fig. 5. Total diatom bloom composition and its temporal distribution. Species density (10^3 cells.L⁻¹) for the ones >5 % of the total diatom abundance on each sample day; relative abundance, indicated with labels, for taxa present in more than 50 % on each sampling day. *P. seriata* = *Pseudo-nitzschia seriata* group; *P. delicatissima* = *Pseudo-nitzschia delicatissima* group. Total diatoms = Diatom abundance (dashed brown line). The numbers on the bars correspond to the chronological order of the blooms. (For interpretation of the references to colour in this figure legend, the reader is referred to the Web version of this article.)

3.3. Species composition of diatom blooms

Eleven of the identified blooms (69 %) showed a dominant species. The most frequently dominant species in bloom conditions were *Pseudo-nitzschia* spp. (25 %), followed by *Leptocylindrus danicus*, *Thalassiosira* spp. and *Chaetoceros* spp. (12.5 % of the blooms each) and *Skeletonema* cf. *costatum* (6 %). *Pseudo-nitzschia* spp. were present in 56 % of the blooms (Figs. 4 and 5). This fact was more evident in 2020, being present in 86 % of the blooms, compared to 33 % observed in 2019.

Overall, the diatom blooms in 2020 exhibited greater abundances than those in 2019. *Chaetoceros* spp. dominant at two autumnal 2020 samples, were present in 86 % of the blooms. In contrast, *Leptocylindrus danicus* constituted a substantial fraction of the assemblage in the majority of 2019 blooms, a pattern not observed during 2020, where it was abundant in a single bloom. *Pseudo-nitzschia* spp. was the dominant taxon in the summer of 2019 and the summer and spring of 2020 blooms. *Detonula pumila*, was never dominant in blooms, but comprised up to 46 % of one. Most remaining cells were composed of *Guinardia delicatula*. These two species, along with unidentified centric diatoms, reached concentrations exceeding 100×10^3 cells.L⁻¹ at one of the blooms (Fig. 5). Although not dominant, these species' presence contributes significantly to the phytoplankton community during the study period.

3.4. Upwelling influence

Persistent negative indices (Fig. 6) show favourable conditions for upwelling from March to October on both the southern and western coasts, with an anomalous event in November 2019. The western coast experienced more intense conditions for upwelling than the southern coast, particularly evident during June, July, and August. Upwelling events were generally pulsed, characterised by intermittent relaxation periods and occasional reversals (Fig. 6). Diatom blooms were typically preceded by wind-induced upwelling conducive conditions to their development for several days (usually exceeding five) (Fig. 6c and d,e). Subsequently, on numerous occasions, blooms dominated by *Leptocylindrus danicus*, or those with high abundances of this species, occurred following relaxation periods or even reversal conditions.

Blooms dominated by *Thalassiosira* spp. (numbers 8 and 9 in Fig. 6) also exhibited this pattern. Blooms of *Pseudo-nitzschia* spp., and samples with high concentrations of these species, were observed on sampling dates coinciding with the onset of relaxation periods and the resumption of upwelling-induced conditions.

A unique episode during the study period highlighted the most intense conditions opposing upwelling, originating along the south coast. Strong south-easterly winds off the south coast resulted in a positive upwelling index of $3.34 \text{ m}^3 \text{ s}^{-1}$ (peak: 27/03/2019, Fig. 6). This positive index indicates rather intense non-upwelling conditions likely creating favourable circumstances for downwelling. Before this event, conditions conducive to intense upwelling had occurred, typically providing the conditions for diatoms to develop.

3.5. Toxic diatom events

Pseudo-nitzschia H. Peragallo was the sole toxic diatom genus capable of forming HABs detected in this study. The abundance of this genus exhibited a higher correlation with Chla concentration than that of other diatoms as demonstrated by a statistically significant, positive and strong correlation with Chla (Spearman's $\rho = 0.636$; $p < 0.001$), stronger than the correlation observed between Chla and total diatom abundance.

This study recorded *Pseudo-nitzschia* spp. cell abundances exceeding the alert threshold of 100×10^3 cells.L⁻¹ by the IPMA SNMB on four sampling dates in 2019 and in six in 2020. Most sampling days with *Pseudo-nitzschia* spp. abundances above the alert threshold coincided with diatom bloom conditions. In 2019, seasonal exceedances of this threshold were observed in spring, summer (twice, probably a single event), and autumn. In 2020, exceedances occurred three times in spring (probably two events), once in summer, and twice in autumn.

DA concentrations in bivalves tissues measured by IPMA on samples corresponding to our sample dates exceeding abundance thresholds were significantly below the regulatory limit of 20 mg DA Kg⁻¹ wet weight of shellfish tissue (Table 2; IPMA, 2022).

However, a review of all toxin values published by IPMA, revealed one instance exceeding the regulatory threshold. This occurred on 02.04.2019 within the study period and in the corresponding bivalve

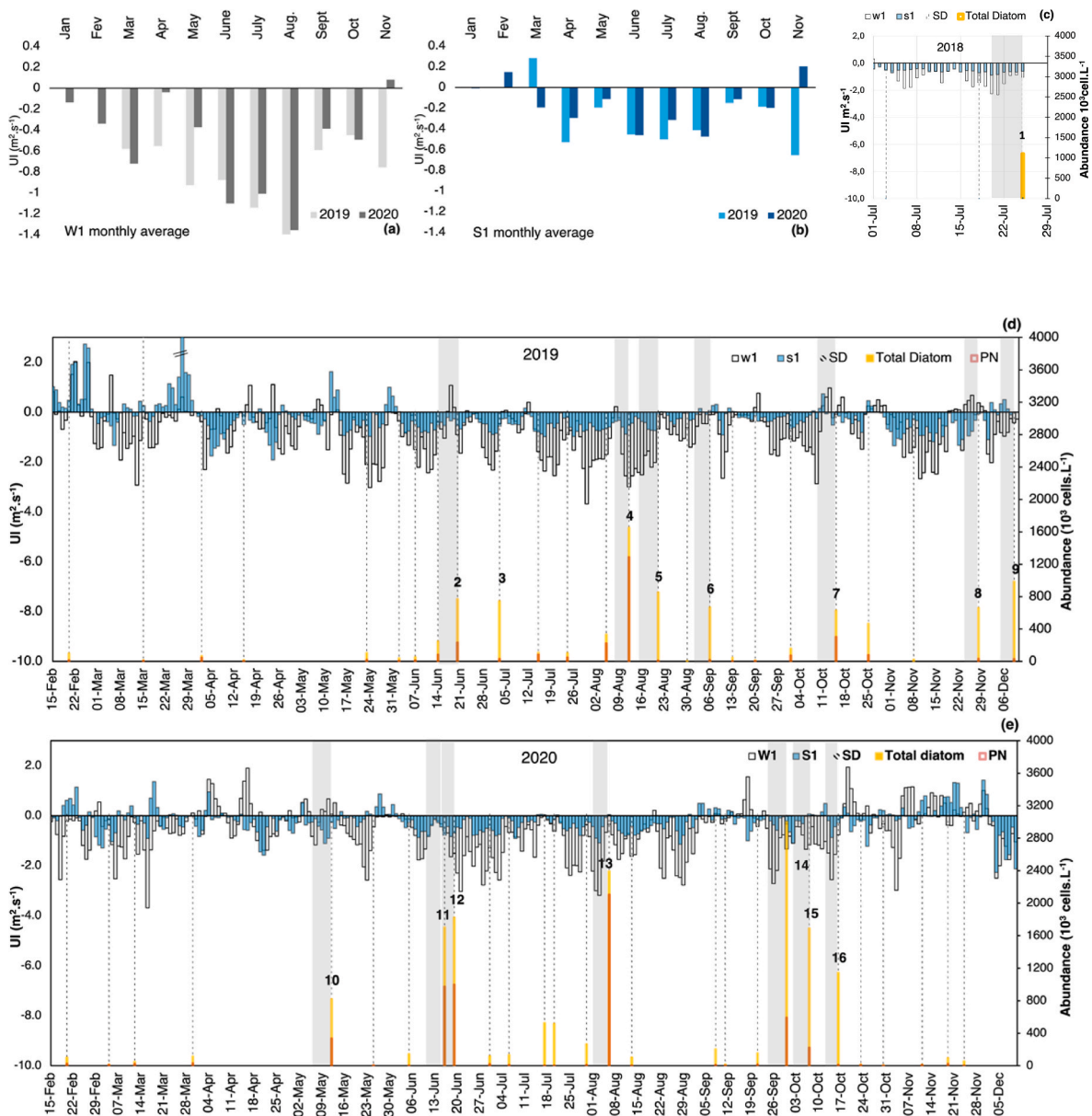


Fig. 6. Temporal distribution of monthly average upwelling index (UI) in 2019 and 2020: (a) on the west coast; (b) on the south coast. Temporal distribution of daily upwelling index (UI in $\text{m}^3 \cdot \text{s}^{-1}$) vs. diatom abundance ($10^3 \text{ cells} \cdot \text{L}^{-1}$) during (c) 2018; (d) 2019; and (e) 2020. W1 - daily upwelling index on the west coast ($\text{m}^3 \cdot \text{s}^{-1}$); S1 - daily upwelling index on the south coast ($\text{m}^3 \cdot \text{s}^{-1}$); SD - sampling date. Yellow bars represent total diatom (diatom abundance), and red bars represent the abundance of *Pseudo-nitzschia* spp. The numbers identify the blooms. Grey rectangles indicate 5 days before sampling dates corresponding to diatom blooms. Negative values of the index indicate upwelling. (For interpretation of the references to colour in this figure legend, the reader is referred to the Web version of this article.)

production area (L7c1). The recorded concentration was 1.5 times the regulatory limit. On this sampling date, *Pseudo-nitzschia* abundance was below alert level, ($44 \times 10^3 \text{ cells} \cdot \text{L}^{-1}$), and, therefore, not included in Table 2. Toxin detection in bivalve tissues coincided with *Pseudo-nitzschia seriata* group abundances exceeding $33 \times 10^3 \text{ cells} \cdot \text{L}^{-1}$ in the IPMA database. In this study, *Pseudo-nitzschia* from the *seriata* group was the only identified on the sample date coinciding with the toxin regulatory limit surpassed. *Pseudo-nitzschia australis* was the most probable species (data not shown). This identification, however, relied solely on inverted microscopy, introducing potential accuracy concerns. Another production area, (L7c2) on the south coast of Portugal, contiguous to L7c1 also exhibited toxicity surpassing the regulatory limit for toxins in the IPMA database in 01.04.2019.

The Harmful Algal Information System (IOC-UNESCO, 2022) - HAEDAT database - didn't record ASP events for the corresponding area

of the study (L7c1). In the nearest area, "Lagos Coastal, South Coast HAB Area" (code Pt-06) (L7c2), two ASP-associated events resulted in the suspension of bivalve harvesting in the coastal production area for the period in study. The first event, attributed to shellfish toxins, led to closures from 04.04.2019 to 18.04.2019. The second event involved high concentrations of the *Pseudo-nitzschia seriata* group, reaching $348500 \text{ cells} \cdot \text{L}^{-1}$ on 05.08.2019. Although no toxicity was detected, this led to closures from 09.08.2019 to 29.08.2019. According to the same database, during the analysed period, for L7c2, there were 591 days of bivalve harvesting closures related to DSP syndrome, 38 days related to PSP syndrome, and 34 days related to ASP syndrome.

4. Discussion

The planktonic diatoms identified at the sampling site off Sagres

Table 2

Sample dates where *Pseudo-nitzschia* abundances exceeded IPMA SNMB thresholds. *Pseudo-nitzschia* spp. (*P.*) aboveundance above the alert level ($>100 \times 10^3$ cells.L⁻¹); *Pseudo-nitzschia delicatissima* (*P.d*) and *Pseudo-nitzschia seriata* (*P.s*) groups above warning thresholds (500×10^3 cells.L⁻¹ and 80×10^3 cells.L⁻¹, respectively) and above closure thresholds (1×10^5 cells.L⁻¹ and 200×10^3 cells.L⁻¹, respectively). When the alert level is not surpassed, the threshold is indicated. Exceedances of closure values are shown in **bold**. *Pseudo-nitzschia* spp. abundances reported by IPMA for proximate dates and the corresponding area (L7c1) within its SNMB. AST: ASP toxin concentration from the analysis in Bivalves; in parentheses: the dates in the final columns indicate the closest date from IPMA abundances and to IPMA measured toxin levels. NQ: not quantified * Data accessed at <https://www.ipma.pt/>.

Sample dates	Season	Abundance (in cells.L ⁻¹)		ASP producer > alert threshold	ASP producers from IPMA SNMB for similar dates*	Analysed bivalve *	AST by IPMA SNMB in L7c1* (mg/kg)*
		<i>P.d</i> in this study > warning/closure threshold	<i>P.s</i> in this study > warning/closure threshold				
20.06.2019	Spring	$\leq 500 \times 10^3$	91×10^3	232806	61910 (17.06.2019)	–	NQ (20.06.2019) 2 (25.06.2019)
05.08.2019	Summer	$\leq 500 \times 10^3$	$\leq 80 \times 10^3$	221720	257890	<i>Mytilus</i> spp.	NQ (05.08.2019)
12.08.2019	Summer	1222 x 10³	$\leq 80 \times 10^3$	1286900	607620	<i>Mytilus</i> spp.	3 (12.08.2019)
15.10.2019	Autumn	$\leq 500 \times 10^3$	$\leq 80 \times 10^3$	301785	272650 (07.10.2019)	–	NQ (14.10.2019)
12.05.2020	Spring	$\leq 500 \times 10^3$	217 x 10³	332826	73800	–	5 (12.05.2020)
16.06.2020	Spring	872×10^3	101×10^3	972899	903640 (15.06.2020)	<i>Mytilus</i> spp.	NQ (15.06.2020)
19.06.2020	Spring	866×10^3	129×10^3	995500	542840 (22.06.2020)	<i>Mytilus</i> spp.	NQ (17.06.2020) NQ (22.06.2020)
06.08.2020	Summer	2042 x 10³	$\leq 80 \times 10^3$	2104660	360 (03.08.2020) 34400 (18.08.2020)	<i>Crassostrea</i> spp.	NQ (03.08.2020) 2.04 (18.08.20)
30.09.2020	Autumn	507×10^3	85×10^3	591500	12120 (27.09.2020)	<i>Mytilus</i> spp.	NQ (27.09.2020)
07.10.2020	Autumn	$\leq 500 \times 10^3$	$\leq 80 \times 10^3$	222194	116030 (05.10.2020) 16810 (12.10.2020)	<i>Mytilus</i> spp.	NQ (05.10.2020) NQ (12.10.2020)

greatly contribute to primary productivity, particularly under bloom conditions, although the nanoflagellates are numerically dominant. This was evidenced by the increase in both absolute cell density and relative proportion of diatoms within the total phytoplankton community during periods of high phytoplankton biomass. Furthermore, the strong positive correlation between diatom abundance and Chl_a concentration, in contrast to the non-significant correlation observed for nanoflagellates, reinforces the substantial contribution of diatoms to phytoplankton biomass and, consequently, productivity. These findings are consistent with those of Icelly et al. (2013) and Goela et al. (2014) for the same area, suggesting stability in abundance patterns over time. Other studies (e.g., Loureiro et al., 2008; Goela et al., 2015) also highlighted the importance of diatoms in this region. The stronger correlation between diatom abundance and Chl_a concentration observed in the study, compared to a previous analysis (Danchenko et al., 2019), does not necessarily indicate an increasing importance of diatoms. This difference is more likely attributable to the larger dataset employed in the present study, rather than a genuine increase in diatom dominance. Therefore, further research is required to evaluate potential long-term shifts in their relative importance.

The maximum annual diatom abundance in 2019 was considered high when compared to other locations, but similar to values reported for nearby locations in previous studies (e.g. Loureiro et al., 2005; Danchenko et al., 2019). In 2020, this maximum nearly doubled. There was some interannual variability, however not explained based on available data. The maximum in 2020 occurred at a slightly different time of year than usual, as instead of the typical spring-summer maximum (Moita, 2001), it was observed in autumn. Frequent intense diatom blooms, occurring across multiple seasons (spring/summer/autumn), potentially benefited mussel growth and productivity for a significant portion of the year. Diatom blooms typically align with the regional upwelling period (April–October), though in 2019, upwelling extended into late November and early December.

The increased diatom abundance observed during periods of intense upwelling is consistent with prior investigations (Abrantes and Moita, 1999; Loureiro et al., 2005; Icelly et al., 2013; Goela et al., 2014, 2015; Danchenko et al., 2019). This can be attributed to their comparatively rapid reproductive rates relative to other phytoplankton taxa, in addition to their physiological adaptation to turbulent hydrodynamic conditions. These characteristics confer a competitive advantage during upwelling events, enabling them to efficiently utilise the elevated

nutrient concentrations characteristically associated with such phenomena.

The influence of upwelling on diatom assemblages during bloom events is evident, with all dominant taxa observed in these blooms characteristic of upwelling conditions. This observation aligns with other researchers' findings who also reported these taxa following upwelling-induced conditions. Examples include *Pseudo-nitzschia* spp. (Moita, 2001; Loureiro et al., 2005; Lassiter et al., 2006; Trainer et al., 2010), *Chaetoceros* spp., *Thalassiosira* spp. (e.g., Moita, 2001; Loureiro et al., 2005), *Skeletonema* cf. *costatum* and *Leptocylindrus danicus*. The latter species is classified as belonging to the second stage of upwelling, as it is less well-adapted to turbulence (Silva et al., 2009). This is consistent with our detection of *Leptocylindrus danicus* following prolonged upwelling conducive conditions, succeeded by a relaxation period. Regarding *Skeletonema* cf. *costatum*, species of this genus are less frequently observed in blooms by other authors; however, it has been previously reported at least once in a diatom bloom within an upwelling centre in the northwestern Iberian Peninsula, which occurred in winter (Álvarez-Salgado et al., 2005).

The data suggest that upwelling conducive conditions along the west coast are more relevant than those from the south coast, as indicated in previous studies (Goela et al., 2016; Krug et al., 2017). However, the methodology used, based on UI, doesn't allow for confirmation of each favourable condition, based on the effective formation of upwelling along the southwest coast due to windstress curl. This phenomenon is a consequence of upwelling conducive conditions on the west coast. Diatom blooms were associated with upwelling conditions occurring within a week, rarely persisting longer. Unlike the persistent upwelling along the western Iberian coast, the southern Portuguese coast experiences episodic upwelling events lasting only a few days (De Oliveira Júnior et al., 2022). Some of the observed diatom blooms occurring after upwelling conducive conditions on the west coast are probably formed due to the water enrichment from upwelling in the west coast, summed with that from upwelling originating along the southwest coast. In two instances, blooms initiated by brief west coast upwelling and persisted due to subsequent upwelling on the southern coast, a pattern distinct from other Iberian locations such as Lisbon Bay (Silva et al., 2009). Determining the precise lag between the onset of upwelling on the coast and the subsequent diatom bloom remains challenging, as sampling may not always coincide with bloom initiation. However, our analysis suggests a general lag of some days between upwelling-favourable winds

and observed blooms, consistent with previous studies (e.g. Goela et al., 2016). Although most of the observed diatom blooms might be explained by upwelling, wind conditions conducive to upwelling did not always result in diatom blooms, as diatom populations may have been limited by other factors such as light intensity, temperature, salinity, herbivory and currents, despite the increased nutrients that upwelling potentially brings.

Cylindrotheca closterium, a frequent benthic diatom in the study area, only reached high densities in one instance, likely due to resuspension caused by turbulence. This species, along with *Pseudo-nitzschia* spp., was previously identified as dominant in microcosm studies from nearby waters (Edwards et al., 2005). From an applied perspective, *Cylindrotheca closterium* and *Skeletonema* cf. *costatum* are widely cultivated for aquaculture, particularly for shrimp, oysters, and other filter feeders (Li et al., 2021; Van Houcke et al., 2017). The observed occurrence of late season blooms, including those from these species, could thus have positive implications for offshore non-fed aquaculture. However, it remains uncertain whether this pattern will persist in the future.

Chaetoceros spp. is frequently dominant during summer along the Portuguese coast (Moita, 2001); however, high densities were recorded here only in spring and autumn 2020. These differences may be because the species within the genus may have changed.

Concerns regarding toxin concentration originating from the diatom community, particularly from the genus *Pseudo-nitzschia*, are valid, as this genus is a known producer of ASP toxins, but somewhat limited. *Pseudo-nitzschia* was indeed the most dominant, abundant, and frequent diatom taxon during the study period. However, its abundance strongly correlated with Chla levels, reinforcing its importance for diatom productivity. This was so relevant that it was even stronger than the correlation between Chla and total diatoms. *Pseudo-nitzschia* abundance like that previously referred to by other authors is strongly linked to upwelling events in this region (Goela et al., 2015; Danchenko et al., 2019; Lima et al., 2022). Also, this taxon was abundant from spring to autumn, coinciding with the known period of ASP toxin production along the Portuguese coast (Vale et al., 2008). DA concentration within bivalve tissues during this study did not correlate with *Pseudo-nitzschia* abundance, with this neurotoxin consistently registering at low levels, except for one sample date. This observation can be explained by the understanding that not all *Pseudo-nitzschia* species biosynthesise substantial concentrations of toxins. In general terms, *Pseudo-nitzschia* species belonging to the *seriata* group demonstrate a greater propensity for DA production. In contrast, those within the *delicatissima* group are associated with a lower degree of toxicity (Fernandes-Salvador et al., 2021). For instance, *P. multiseriata*, *P. seriata*, and *P. australis* exhibit comparatively elevated DA production, and species such as *P. delicatissima* and *P. pseudodelicatissima* typically produce lower concentrations of this toxin, except for *P. fraudulenta*, which, despite being in the *seriata* group, is not a prolific producer (Lundholm et al., 2002). Palenzuela et al. (2019) also demonstrated in the Galician Rías that *Pseudo-nitzschia* abundances were not invariably linked to DA concentrations. Along the Portuguese coast, *Pseudo-nitzschia australis* Freguelli (*seriata* group) has been the species implicated in the presence of DA (Palma et al., 2010; Vale and Sampayo, 2001). The proportional abundance of the *seriata* group within the total *Pseudo-nitzschia* population was generally low in our study. Moreover, the sole instance of DA exceeding regulatory thresholds in bivalve tissues coincided with a *Pseudo-nitzschia* community solely represented by the *seriata* group, likely *P. australis*. This suggests that blooms of the *P. delicatissima* group, even at high cell densities, pose a comparatively lower risk than those dominated by the *seriata* group. Given that DA levels recorded above the closure limit for the Portuguese coast were largely absent between 1986 and 2006 (Vale et al., 2008), and continued to be infrequent until 2020, with no reported ASP incidents in humans (Vale et al., 2008; Vale, 2022), it would therefore likely be more efficacious, in the short term, to focus monitoring efforts on elucidating the environmental conditions that may precipitate the production of DA by the *seriata* group,

principally *P. australis*. Despite the low risk of ASP in humans within this region, economic disruption from harvesting closures exists not only locally but also in various other geographical areas worldwide (Trainer et al., 2011). That could be minimized with better predictions.

Another possible explanation for toxin levels in bivalves not being so high in this area, despite elevated densities of the potential DA producer *Pseudo-nitzschia*, may be the high hydrodynamics, evidenced by several studies (de Oliveira Júnior et al., 2021, 2022, 2024). The eventual toxin-producing diatoms transported by the upwelled water flowing eastward might have short residence time to be available for bivalves. Thus, toxins do not accumulate significantly (Davidson et al., 2016). On the other hand, DA levels decrease rapidly in bivalve tissue, when they are no longer exposed to the toxin (Vale and Sampayo, 2001). Also, the mussel *Mytilus galloprovincialis* is known to eliminate DA more rapidly than other bivalves (Blanco et al., 2002).

A singular instance of elevated DA concentration in this study (the sole instance exceeding regulatory limits) coincided with unique southeasterly conditions on the south coast, resulting in exceptionally intense conditions opposing upwelling formation. This wind event occurred following a period of conditions conducive to upwelling on the west coast. Although this isolated occurrence does not constitute definitive evidence for DA formation, this hypothesis warrants exploration in future studies. This is plausible as these conditions could facilitate the accumulation of toxin-producing diatoms near the bivalve farm via downwelling, allowing the bivalves sufficient contact time to accumulate toxins if produced. Downwelling is frequently associated with such wind patterns. Also, immediately before this, conducive upwelling conditions had been present, which typically promote diatom proliferation. If downwelling occurred when ASP producer cells were present in large numbers, this could lead to a subsequent accumulation of diatom cells in the vicinity of the aquaculture site, potentially leading to the concentration of DA in bivalves if produced. Furthermore, the likely concurrent counter-current could have elevated water temperatures (Relvas and Barton, 2002; de Oliveira Júnior et al., 2022, 2024), potentially triggering toxin production. Higher temperatures, beyond the optimal range, are indicated to trigger DA production in *Pseudo-nitzschia australis* (Thorel et al., 2014). Other studies have indicated that during upwelling relaxation events, *Pseudo-nitzschia* cells are predominantly concentrated in nearshore waters, with a gradual decline observed further offshore (Du et al., 2016). It is noteworthy that our sampling point is located relatively close to the shore, less than a nautical mile away. Previous studies, such as that of Álvarez-Salgado et al. (2005) have also reported the development of blooms of *Pseudo-nitzschia australis* following upwelling relaxation events in Monterey Bay, on the coast of California. On the other hand, also Loureiro et al. (2011) referred to the possibility of the formation of retention sites around the CSV upwelling centre, which may contribute to the local accumulation of harmful species. This is also consistent with Lima et al. (2022), who, drawing on the work of Hickey et al. (2013), Giddings et al. (2014), and McCabe et al. (2016), noted that during the upwelling season, intermittent sequences of upwelling followed by relaxation or downwelling events promote the accumulation of phytoplankton cells in nearshore areas in this region.

For *Pseudo-nitzschia australis* densities to become problematic, these specific conditions are necessary: sufficient light intensity, optimal temperature, and adequate nutrients, including silica. Predation by copepods also trigger DA production (Zhang et al., 2021).

There were two instances (Summer of 2019 and Summer of 2020) of *P. delicatissima* group blooms, where their concentration was above the closure level, but *P. seriata* group didn't even reach the alert level. Yet, toxins were found in the shellfish. However, the toxin levels were, at least, seven times lower than what's legally allowed, and the *P. seriata* group abundance was 64900 and 62660 in 2019 and 2020, respectively. This suggests that, even without high *P. seriata* abundances, their blooms can lead to detectable toxins in shellfish, although at considerably lower concentrations than the regulatory limit.

5. Conclusions

The questions posed at the end of introduction were answered through four indicators: the contribution of diatom abundance to phytoplankton productivity (here considering the biomass proxy, Chla), the relationship between upwelling events and diatom blooms, the frequency and intensity of these blooms, and the relevance of potential toxin producers within the diatom community. Three of the four questions were confirmed, as expected; however, the significance of the potential toxin-producer *Pseudo-nitzschia* was greater than anticipated: *Pseudo-nitzschia* was the most abundant, dominant, and frequent taxon during the study period and within bloom assemblages. Despite frequent HABs from this genus, no concerning toxin levels were detected in the study area during diatom blooms. In fact, DA concentrations in bivalve tissues exceeded regulatory limits only once. In this case, it coincided with the presence of the *Pseudo-nitzschia seriata* group (likely *Pseudo-nitzschia australis*), although below the regulatory limit, and in the absence of the *Pseudo-nitzschia delicatissima* group. This suggests that the prominence of *Pseudo-nitzschia* species, particularly the *delicatissima* group, is acceptable, whereas the less represented *seriata* group may pose a toxin risk even at lower abundances than the regulatory levels.

Based on this analysis, the following site suitability criteria can here be proposed:

- A strong positive correlation between Chla and diatom abundance (stronger than for other phytoplankton groups).
- Identification of bloom origins in upwelling events, indicated by wind-stress indices.
- Frequent, high-abundance diatom blooms occur throughout much of the year.
- Minimal significance of potential toxin producers (included a great abundance of those species that, although dominant, are not linked to DA production).

It was shown that the development of *Pseudo-nitzschia* is associated with the occurrence of AST between spring and autumn. It was linked with the occurrence of the sole DA surpassing regulatory limits as well as specific oceanographic conditions. These were strong upwelling conditions originating on the west coast followed by their relaxation, succeeded by strong opposite conditions originating on the south coast, persisting for more than 10 days. Could this represent necessary conditions for DA occurrence at this location? This requires further confirmation and depends on additional factors such as light and temperature, but it also can be used for further research evaluation.

For future work, increased sampling during winter and autumn is recommended to address seasonal gaps. Additionally, identifying the specific *Pseudo-nitzschia* species present is crucial. Focusing on the species responsible for DA production, rather than the entire genus, would enhance resource allocation and improve risk mitigation. Future research could incorporate upwelling indices from both the west and south coasts into machine learning predictive models - already used in this area with success (O'Donncha et al., 2024) to forecast the timing most favourable for the accumulation of ASP toxins in bivalves. Detecting the conditions for toxin production before accumulation in bivalves would be a valuable tool for aquaculture management and development of the Blue Economy.

The methodology used here, by incorporating frequent phytoplankton samples combined with upwelling indices, can be adapted to other sites where bivalve production is located at upwelling dependent regions. It facilitates the selection of suitable sites for new bivalve aquaculture installations, optimising monitoring programmes, and the minimisation of excessive closures of bivalve harvesting. Also, investigating local public data allows for the inference of the absence of frequent toxicity caused by diatoms in bivalves. With this strategy, monitoring efforts can be refined to focus on the organism in question rather than the broader genus. Additionally, artificial intelligence

predictive models could integrate the presence of this specific diatom to forecast bivalve toxicity more accurately.

CRediT authorship contribution statement

Carla S. Freitas: Writing – original draft, Methodology, Investigation, Formal analysis, Conceptualization. **Priscila Goela:** Writing – review & editing, Supervision, Methodology, Conceptualization. **John Icely:** Writing – review & editing. **Bruno D.D. Fragoso:** Writing – review & editing, Methodology, Formal analysis, Data curation. **Luciano de Oliveira Júnior:** Writing – review & editing, Methodology, Formal analysis. **Sónia Cristina:** Writing – review & editing, Supervision. **Alice Newton:** Writing – review & editing, Supervision.

Author agreement statement

The authors declare that this manuscript is original, has not been published before and is not currently being considered for publication elsewhere. The authors confirm that the manuscript has been read and approved by all named authors and that there are no other persons who satisfied the criteria for authorship but are not listed. We further confirm that the order of authors listed in the manuscript has been approved by all of us. We understand that the Corresponding Author is the sole contact for the Editorial process. She is responsible for communicating with the other authors about progress, submissions of revisions and final approval of proofs.

Declaration of competing interest

The authors declare that they have no known competing financial interests or personal relationships that could have appeared to influence the work reported in this paper.

Acknowledgements

The authors wish to acknowledge the financial support provided by the Portuguese Foundation for Science and Technology (FCT) to CIMA through <https://doi.org/10.54499/UIDB/00350/2020> and through project <https://doi.org/10.54499/LA/P/0069/2020> award to the Associated laboratory ARNET. Carla Freitas received support from FCT via the PhD fellowship <https://doi.org/10.54499/UI/BD/151429/2021>. Sónia Cristina's work was funded by the program contract - CEECINSTLA/00018/2022 for the performance of research activities at CIMA under the scope of the Associated Laboratory ARNET (LA/P/0069/2020). Luciano de Oliveira Junior was supported by FCT through a PhD fellowship SFRH/BD/140250/2018. Priscila Goela was financed through FCT under the grant CEECIND/02014/2017 during part of the activities of this work and it is currently funded by S2AQUA - Collaborative Laboratory, Association for a Sustainable and Smart Aquaculture, through Missão Interface, a project co-funded by PRR - Recovery and Resilience Plan by European Commission (operation code 01/C05-i02/2022.P148). John Icely and Bruno Fragoso received funding from Sagremarisco, Lda. and received support under the GAIN - Green Aquaculture Intensification in Europe project, funded by the European Union's Horizon 2020 Research and Innovation Programme (grant agreement no. 773330) contributing to the collection of samples and data used for the development of this work and the Horizon Europe NOVAFOODIES project, under grant agreement 101084180. Alice Newton acknowledges Future Earth Coasts and IMBeR.

We want to acknowledge Project GAIN, for its support in facilitating sampling and data collection. Additionally, the authors also want to thank the Instituto Português do Mar e da Atmosfera. I.P. (IPMA) for access to its public database of the SNMB, Copernicus Climate Change Service for providing the wind data and to IOC-UNESCO Harmful Algae Information System (HAIS).

Appendix A. Supplementary data

Supplementary data to this article can be found online at <https://doi.org/10.1016/j.marenvres.2025.107200>.

Data availability

Data will be made available on request.

References

- Abrantes, F., Moita, M.T., 1999. Water column and recent sediment data on diatoms and coccolithophorids, off Portugal, confirm record of upwelling events. *Oceanol. Acta* 22 (1), 67–84. [https://doi.org/10.1016/S0399-1784\(99\)80034-6](https://doi.org/10.1016/S0399-1784(99)80034-6).
- Alvarez, I., Gomez-Gesteira, M., deCastro, M., Dias, J.M., 2008. Spatiotemporal evolution of upwelling regime along the western coast of the Iberian Peninsula. *J. Geophys. Res.* Oceans 113 (7). <https://doi.org/10.1029/2008JC004744>.
- Álvarez-Salgado, X.A., Nieto-Cid, M., Piedracoba, S., Crespo, B.G., Gago, J., Brea, S., Teixeira, I.G., Figueiras, F.G., Garrido, J.L., Rosón, G., Castro, C.G., Gilcoto, M., 2005. Origin and fate of a bloom of *Skeletonema costatum* during a winter upwelling/downwelling sequence in the Ría de Vigo (NW Spain). *J. Mar. Res.* 63 (6), 1127–1149. <https://doi.org/10.1357/002224005775247616>.
- Avdelas, L., Avdic-Mravljje, E., Borges Marques, A.C., Cano, S., Capelle, J.J., Carvalho, N., Cozzolino, M., Dennis, J., Ellis, T., Fernández Polanco, J.M., Guillen, J., Lasner, T., Le Bihan, V., Llorente, I., Mol, A., Nicheva, S., Nielsen, R., van Oostenbrugge, H., Villasante, S., Visnic, S., Zhelev, K., Asche, F., 2021. The decline of mussel aquaculture in the European Union: causes, economic impacts and opportunities. *Rev. Aquacult.* 13 (1), 91–118. <https://doi.org/10.1111/RAQ.12465>.
- Bach, L., Taucher, J., 2019. CO₂ effects on diatoms: a synthesis of more than a decade of ocean acidification experiments with natural communities. *Ocean Sci.* 15 (4), 1159–1175. <https://doi.org/10.5194/OS-15-1159-2019>.
- Bakun, A., 1973. Coastal upwelling indices, west coast of North America, 1946–71. <http://repository.library.noaa.gov/view/noaa/9041>.
- Blanco, J., Bermúdez De La Puente, M., Arévalo, F., Salgado, C., Morono, Á., 2002. Depuration of mussels (*Mytilus galloprovincialis*) contaminated with domoic acid. *Aquat. Living Resour.* 15 (1), 53–60. [https://doi.org/10.1016/S0990-7440\(01\)01139-1](https://doi.org/10.1016/S0990-7440(01)01139-1).
- Boyce, D.G., Lewis, M.R., Worm, B., 2010. Global phytoplankton decline over the past century. *Nature* 2010 466 (7306), 591–596. <https://doi.org/10.1038/nature09268>.
- Camacho, A.P., Labarta, U., Beiras, R., 1995. Growth of mussels (*Mytilus edulis galloprovincialis*) on cultivation rafts: influence of seed source, cultivation site and phytoplankton availability. *Aquaculture* 138 (1–4), 349–362. [https://doi.org/10.1016/0044-8486\(95\)01139-0](https://doi.org/10.1016/0044-8486(95)01139-0).
- CEN, 2006. EN 15204:2006 - Water Quality - Guidance Standard on the Enumeration of Phytoplankton Using Inverted Microscopy (Utermöhl Technique). Comité Européen de Normalisation. <https://www.ipq.pt/normalizacao/normas/>.
- CEN, 2011. EN 15972:2011. Water Quality - Guidance on Quantitative and Qualitative Investigations of Marine Phytoplankton. Comité Européen de Normalisation. <https://www.ipq.pt/normalizacao/normas/>.
- Cohen, J., 1992. Statistical power analysis. *Curr. Dir. Psychol. Sci.* 1 (3), 98–101. <https://doi.org/10.1111/1467-8721.ep10768783>.
- Cravo, A., Relvas, P., Cardeira, S., Rita, F., 2013. Nutrient and chlorophyll a transports during an upwelling event in the NW margin of the Gulf of Cadiz. *J. Mar. Syst.* 128, 208–221. <https://doi.org/10.1016/J.JMARSYS.2013.05.001>.
- Cravo, A., Relvas, P., Cardeira, S., Rita, F., Madureira, M., Sánchez, R., 2010. An upwelling filament off southwest Iberia: effect on the chlorophyll a and nutrient export. *Cont. Shelf Res.* 30 (15), 1601–1613. <https://doi.org/10.1016/J.CSR.2010.06.007>.
- Cropper, T.E., Hanna, E., Bigg, G.R., 2014. Spatial and temporal seasonal trends in coastal upwelling off Northwest Africa, 1981–2012. *Deep Sea Res. Oceanogr. Res. Pap.* 86, 94–111. <https://doi.org/10.1016/J.DSR.2014.01.00>.
- Danchenko, S., Dodge, J.D., Icelly, J.D., Newton, A., 2022. Dinoflagellate assemblages in the west Iberian upwelling region (Sagres, Portugal) during 1994–2001. *Front. Mar. Sci.* 9, 591759. <https://doi.org/10.3389/fmars.2022.591759>.
- Danchenko, S., Frago, B., Guillebault, D., Icelly, J., Berzano, M., Newton, A., 2019. Harmful phytoplankton diversity and dynamics in an upwelling region (Sagres, SW Portugal) revealed by ribosomal RNA microarray combined with microscopy. *Harmful Algae* 82, 52–71. <https://doi.org/10.1016/J.HAL.2018.12.002>.
- Davidson, K., Anderson, D.M., Mateus, M., Reguera, B., Silke, J., Sourisseau, M., Maguire, J., 2016. Forecasting the risk of harmful algal blooms. *Harmful Algae* 53, 1–7. <https://doi.org/10.1016/J.HAL.2015.11.005>.
- De Oliveira Júnior, L., Garel, E., Relvas, P., 2021. The structure of incipient coastal counter currents in South Portugal as indicator of their forcing agents. *J. Mar. Syst.* 214, 103486. <https://doi.org/10.1016/J.JMARSYS.2020.103486>.
- De Oliveira Júnior, L., Relvas, P., Garel, E., 2022. Kinematics of surface currents at the northern margin of the Gulf of Cadiz. *Ocean Sci.* 18 (4), 1183–1202. <https://doi.org/10.5194/egusphere-2022-112>.
- De Oliveira Júnior, L., Relvas, P., Garel, E., 2024. Upwelling processes variability and water circulation along the northern margin of the Gulf of Cadiz. *Cont. Shelf Res.* 281, 105310. <https://doi.org/10.1016/J.CSR.2024.105310>.
- Du, X., Peterson, W., Fisher, J., Hunter, M., Peterson, J., 2016. Initiation and development of a toxic and persistent *pseudo-nitzschia* bloom off the Oregon coast in spring/summer 2015. *PLoS One* 11 (10). <https://doi.org/10.1371/journal.pone.0163977> e 0163977.
- DGRM, 2020. Estratégia marinha para a Subdivisão do Continente. Relatório do 2o ciclo da Directiva Quadro Estratégia Marinha. Parte D - Avaliação do Estado Ambiental. <https://www.dgrm.pt/en/web/guest/as-pem-diretiva-quadro-estrategia-marinha>.
- Edwards, V., Icelly, J., Newton, A., Webster, R., 2005. The yield of chlorophyll from nitrogen: a comparison between the shallow Ria Formosa lagoon and the deep oceanic conditions at Sagres along the southern coast of Portugal. *Estuar. Coast Shelf Sci.* 62 (3), 391–403. <https://doi.org/10.1016/J.ECSS.2004.09.004>.
- European Union, 2017. Regulation 2017/625 of the European Parliament and of the Council of 15 March 2017 on official controls and other official activities performed to ensure the application of food and feed law, rules on animal health and welfare, plant health and plant protection products. *OJ L95* 1–42. <https://eur-lex.europa.eu/legal-content/EN/TXT/?uri=CELEX:32017R0625>.
- FAO, 2022. The State of World Fisheries and Aquaculture 2022. Towards Blue Transformation. FAO, Rome. <https://doi.org/10.4060/CC0461EN>.
- FAO, 2024. The state of World fisheries and aquaculture 2024. In: The State of World Fisheries and Aquaculture 2024 - Blue Transformation in Action. FAO. <https://doi.org/10.4060/CD0683EN>.
- Fernandes-Salvador, J.A., Davidson, K., Sourisseau, M., Revilla, M., Schmidt, W., Clarke, D., Miller, P.I., Arce, P., Fernández, R., Maman, L., Silva, A., Whyte, C., Mateo, M., Neira, P., Mateus, M., Ruiz-Villarreal, M., Ferrer, L., Silke, J., 2021. Current status of forecasting toxic harmful algae for the north-east atlantic shellfish aquaculture industry. *Front. Mar. Sci.* 8, 666583. <https://doi.org/10.3389/FMARS.2021.666583/BIBTEX>.
- Fiuza, A.F.G., de Macedo, M.E., Guerreiro, M.R., 1982. Climatological space and time variation of the Portuguese coastal upwelling. *Acta Oceanologica* 5 (1), 31–40.
- Fragoso, B., Icelly, J., 2009. Upwelling events and recruitment patterns of the major fouling species on coastal J aquaculture (Sagres, Portugal). *J. Coast Res.* 56, 419–423.
- Galparsoro, I., Murillas, A., Pinarbasi, K., Sequeira, A.M., Stelzenmüller, V., Borja, Á., O'Hagan, A.M., Boyd, A., Bricker, S., Garmendia, J.M., Gimpel, A., Gangery, A., Billing, S.L., Bergh, O., Strand, O., Hiu, L., Frago, B., Icelly, J., Ren, J., Papageorgiou, N., Grant, J., Brigolin, D., Pastres, R., Tett, P., 2020. Global stakeholder vision for ecosystem-based marine aquaculture expansion from coastal to offshore areas. *Rev. Aquacult.* <https://doi.org/10.1111/raq.12422>.
- Garel, E., Laiz, I., Drago, T., Relvas, P., 2016. Characterisation of coastal counter-currents on the inner shelf of the Gulf of Cadiz. *J. Mar. Syst.* 155, 19–34. <https://doi.org/10.1016/J.JMARSYS.2015.11.001>.
- Giddings, S.N., MacCreedy, P., Hickey, B.M., Banas, N.S., Davis, K.A., Siedlecki, S.A., Trainer, V.L., Kudela, R.M., Pelland, N.A., Connolly, T.P., 2014. Hindcasts of potential harmful algal bloom transport pathways on the Pacific Northwest coast. *J. Geophys. Res.* Ocean 119, 2439–2461. <https://doi.org/10.1002/2013JC009622>.
- Goela, P.C., Cordeiro, C., Danchenko, S., Icelly, J., Cristina, S., Newton, A., 2016. Time series analysis of data for sea surface temperature and upwelling components from the southwest coast of Portugal. *J. Mar. Syst.* 163, 12–22. <https://doi.org/10.1016/J.JMARSYS.2016.06.002>.
- Goela, P.C., Danchenko, S., Icelly, J.D., Lubian, L.M., Cristina, S., Newton, A., 2014. Using CHEMTAX to evaluate seasonal and interannual dynamics of the phytoplankton community off the South-west coast of Portugal. *Estuar. Coast Shelf Sci.* 151, 112–123. <https://doi.org/10.1016/J.ECSS.2014.10.001>.
- Goela, P.C., Icelly, J., Cristina, S., Danchenko, S., Angel DelValls, T., Newton, A., 2015. Using bio-optical parameters as a tool for detecting changes in the phytoplankton community (SW Portugal). *Estuar. Coast Shelf Sci.* 167, 125–137. <https://doi.org/10.1016/J.ECSS.2015.07.037>.
- Goela, P.C., Icelly, J., Cristina, S., Newton, A., Moore, G., Cordeiro, C., 2013. Specific absorption coefficient of phytoplankton off the Southwest coast of the Iberian Peninsula: a contribution to algorithm development for ocean colour remote sensing. *Cont. Shelf Res.* 52, 119–132.
- Guiry, M. D., Guiry, and G. M., 2024. AlgaeBase. World-Wide electronic publication, university of galway. <https://www.algaebase.org>. (Accessed 31 October 2024).
- Hallegraeff, G.M., Anderson, D., Belin, C., Bottein, M.Y., Bresnan, E., Chinain, M., Enevoldsen, H., Iwataki, M., Karlson, B., McKenzie, C.H., Sunesen, I., Pitcher, G.C., Provoost, P., Richardson, A., Schweibold, L., Tester, P.A., Trainer, V.L., Yñiguez, A. T., Zingone, A., 2021. Perceived global increase in algal blooms is attributable to intensified monitoring and emerging bloom impacts. *Commun. Earth Environ.* 2, 117. <https://doi.org/10.1038/s43247-021-00178-8>.
- Hasle, G.R., 1965. *Nitzschia* and *Fragilariopsis* species studied in the light and electron microscopes. II. The group *Pseudo-nitzschia*. *Det Norske Videnskaps-Akademi i Oslo, I. Mat. Naturv. Klasse, Ny Serie* 18, 1–45.
- Hasle, G.R., Syvertsen, E.E., 1997. Marine diatoms. In: Tomas, C.R. (Ed.), *Identifying Marine Phytoplankton*. Academic Press, pp. 5–385. <https://doi.org/10.1016/B978-012693018-4/50004-5>.
- Hersbach, H., Bell, B., Berrisford, P., Biavati, G., Horányi, A., Muñoz Sabater, J., Nicolas, J., Peubey, C., Radu, R., Rozum, I., Schepers, D., Simmons, A., Soci, C., Dee, D., Thépaut, J.-N., 2023. ERA5 hourly data on single levels from 1940 to present. Copernicus Clim/Change Service (C3S) Climate Data Store (CDS). <https://doi.org/10.24381/cds.adbb2d47>. (Accessed 22 February 2022).
- Hickey, B.M., Trainer, V.L., Michael Kosro, P., Adams, N.G., Connolly, T.P., Kachel, N.B., Geier, S.L., 2013. A springtime source of toxic *Pseudo-nitzschia* cells on razor-clam beaches in the Pacific Northwest. *Harmful Algae* 25, 1–14. <https://doi.org/10.1016/j.hal.2013.01.006>.
- Icelly, J., Frago, B., 2023. Potential effects of climate change on offshore aquaculture of the Mediterranean mussel (*Mytilus galloprovincialis*, Lamarck, 1819) in Portugal. *J. Shellfish Res.* 42 (2), 223–235. <https://doi.org/10.2983/035.042.0204>.

- Icelly, J., Fragoso, B., Moore, Gerald, 2022. Dataset produced by Sagremarisco at Sagres (SW Portugal) pilot site as part of the GAIN project. Zenodo. <https://doi.org/10.5281/zenodo.5874010> [Data set].
- Icelly, J., Moore, G., Danchenko, S., Goela, P., Cristina, S., Zacharias, M., Newton, A., 2013. Contribution of remote sensing products to the management of offshore aquaculture at Sagres, SW Portugal. In: Ouwelhand, Ed. H. (Ed.), Proceedings of ESA Sentinel-3 OLCI/SLSTR and MERIS/(A)ATSR Workshop European Space Agency, p. 6.
- IOC-UNESCO. The Harmful Algal Event database (HAEDAT). Accessed via Harmful Algae Information System. <https://data.hais.ioc-unesco.org/22.10>. (Accessed November 2022).
- IPMA, 2022. Instituto Português do Mar e da Atmosfera. Bivalves. Sistema Nacional de Monitorização de Moluscos Bivalves. Available from: <https://www.ipma.pt/pt/iindex.html>. (Accessed 6 November 2022).
- IPMA, 2013. Plano de Ação-Sistema Nacional de Monitorização de Moluscos Bivalves. Novembro 2013, Available at: https://www.ipma.pt/bin/docs/institucionais/p.accao_smb_2013.pdf.
- Krug, L.A., Platt, T., Sathyendranath, S., Barbosa, A.B., 2017. Unravelling region-specific environmental drivers of phytoplankton across a group marine domain (off SW Iberia). *Rem. Sens. Environ.* 203, 162–184. <https://doi.org/10.1016/j.rse.2017.05.029>.
- Lassiter, A.M., Wilkerson, F.P., Dugdale, R.C., Hogue, V.E., 2006. Phytoplankton assemblages in the CoOP-WEST coastal upwelling area. *Deep Sea Res. Part II Top. Stud. Oceanogr.* 53 (25–26), 3063–3077. <https://doi.org/10.1016/j.dsr2.2006.07.013>.
- Li, H., Xu, T., Ma, J., Li, F., Xu, J., Li, H., Xu, T., Ma, J., Li, F., Xu, J., 2021. Physiological responses of *Skeletonema costatum* to the interactions of seawater acidification and the combination of photoperiod and temperature. *BGeo* 18 (4), 1439–1449. <https://doi.org/10.5194/BG-18-1439-2021>.
- Lima, M.J., Relvas, P., Barbosa, A.B., 2022. Variability patterns and phenology of harmful phytoplankton blooms off southern Portugal: looking for region-specific environmental drivers and predictors. *Harmful Algae* 116, 102254. <https://doi.org/10.1016/j.hal.2022.102254>.
- Lobo, E., Leighton, G., 1986. Estructuras comunitarias de las fitocenosis planctónicas de los sistemas de desembocaduras de ríos y esteros de la zona central de Chile. *Rev. Biol. Mar. Oceanogr.* 22 (1), 1–29. <https://www.scienceopen.com/document?vid=08dd20b1-2647-489c-a640-7f7270e105cf>.
- Lorenzen, C.J., 1967. Determination of chlorophyll and pheo-pigments: spectrophotometric equations. *Limnol. Oceanogr.* 12 (2), 343–346. <https://doi.org/10.4319/LO.1967.12.2.0343>.
- Loureiro, S., Icelly, J., Newton, A., 2008. Enrichment experiments and primary production at Sagres (SW Portugal). *J. Exp. Mar. Biol. Ecol.* 359 (2), 118–125. <https://doi.org/10.1016/j.jembe.2008.03.001>.
- Loureiro, S., Newton, A., Icelly, J.D., 2005. Microplankton composition, production and upwelling dynamics in Sagres (SW Portugal) during summer of 2001. *Sci. Mar.* 69 (3), 323–341. <https://doi.org/10.3989/scimar.2005.69n3323>.
- Loureiro, S., René, A., Garcés, E., Camp, J., Vagué, D., 2011. Harmful algal blooms (HABs), dissolved organic matter (DOM), and planktonic microbial community dynamics at a near-shore and a harbour station influenced by upwelling (SW Iberian Peninsula). *J. Sea Res.* 65 (4), 401–413. <https://doi.org/10.1016/j.jcsr.2012.11.009>.
- Lundholm, N., Churro, C., Escalera, L., Fraga, S., Hoppenrath, M., Iwataki, M., Larsen, J., Mertens, K., Moestrup, Ø., Murray, S., Tillmann, U., Zingone, A. (Eds.), 2009. IOC-UNESCO Taxonomic Reference List of Harmful Micro Algae. <https://doi.org/10.14284/362>. <https://www.marinespecies.org/hab>. (Accessed 22 October 2022).
- Lundholm, N., Daugbjerg, N., Moestrup, Ø., 2002. Phylogeny of the Bacillariaceae with emphasis on the genus *Pseudo-nitzschia* (Bacillariophyceae) based on partial LSU rDNA. *Eur. J. Phycol.* 37 (1), 115–134. <https://doi.org/10.1017/S096702620100347X>.
- Maloy, A.P., Nelle, P., Culloty, S.C., Slater, J.W., Harrod, C., 2013. Identifying trophic variation in a marine suspension feeder: DNA- and stable isotope-based dietary analysis in *Mytilus* spp. *Mar. Biol.* 160 (2), 479–490. <https://doi.org/10.1007/S00227-012-2105-4/FIGURES/7>.
- McCabe, R.M., Hickey, B.M., Kudela, R.M., Lefebvre, K.A., Adams, N.G., Bill, B.D., Gulland, F.M.D., Thomson, R.E., Cochlan, W.P., Trainer, V.L., 2016. An unprecedented coastwide toxic algal bloom linked to anomalous ocean conditions. *Geophys. Res. Lett.* 43 (10), 310–366. <https://doi.org/10.1002/2016GL070023.376>.
- Mascorda-Cabre, L., Sheehan, E.V., Attrill, M.J., Hosegood, P., 2024. Assessing the impact of an offshore longline mussel farm on local water circulation in a highly hydrodynamic energetic bay. *Aquaculture* 585, 740697. <https://doi.org/10.1016/j.aquaculture.2024.740697>.
- Moita, M.T., 2001. Estrutura, variabilidade e dinâmica do Fitoplâncton na Costa de Portugal Continental. University of Lisbon, Portugal.
- Monteiro, H., Goela, P., Pinto, R., Cristina, S., 2024. Harmful Algal Blooms on the Portuguese coast: cross-checking events with remote sensing ocean colour data for coastal management. *Regional Stud. Marine Sci.* 77, 103723. <https://doi.org/10.1016/j.rsmas.2024.103723>.
- Muñiz, O., Revilla, M., Rodríguez, J.G., Laza-Martínez, A., Fontán, A., 2019. Annual cycle of phytoplankton community through the water column: study applied to the implementation of bivalve offshore aquaculture in the southeastern Bay of Biscay. *Oceanologia* 61 (1), 114–130. <https://doi.org/10.1016/J.OCEANO.2018.08.001>.
- O'Donncha, F., Akhriev, A., Fragoso, B., Icelly, J., 2024. Forecasting closures on shellfish farms using machine learning. *Aquac. Int.* 32, 5603–5623. <https://doi.org/10.1007/s10499-024-01438-y>.
- Palma, S., Mourão, H., Silva, A., Barão, M.I., Moita, M.T., 2010. Can *Pseudo-nitzschia* blooms be modeled by coastal upwelling in Lisbon Bay? *Harmful Algae* 9 (3), 294–303. <https://doi.org/10.1016/j.hal.2009.11.006>.
- Palenzuela, J.M.T., Vilas, L.G., Bellas, F.M., Garet, E., González-Fernández, Á., Spyarakos, E., 2019. *Pseudo-nitzschia* blooms in a coastal upwelling system: remote sensing detection, toxicity and environmental variables. *Water* 2019 11 (9). <https://doi.org/10.3390/W11091954>, 1954.
- Parsons, T.R., Maita, Y., Lalli, C.M., 1984. *A Manual of Chemical and Biological Methods for Seawater Analysis*, vol. 173.
- Pernet, F., Malet, N., Pastoureaud, A., Vaquer, A., Quéré, C., Dubroca, L., 2012. Marine diatoms sustain growth of bivalves in a Mediterranean lagoon. *J. Sea Res.* 68, 20–32. <https://doi.org/10.1016/j.seares.2011.11.004>.
- Pronker, A.E., Nevejan, N.M., Peene, F., Geijssen, P., Sorgeloos, P., 2008. Hatchery broodstock conditioning of the blue mussel *Mytilus edulis* (Linnaeus 1758). Part I. Impact of different micro-algae mixtures on broodstock performance. *Aquac. Int.* 16 (4), 297–307. <https://doi.org/10.1007/S10499-007-9143-9/FIGURES/4>.
- Ramos, A., Pires, A., Sousa, P., Trigo, R., 2013. The use of circulation weather types to predict upwelling activity along the western Iberian Peninsula coast. *Cont. Shelf Res.* 69, 38–51. <https://doi.org/10.1016/j.csr.2013.08.019>.
- Relvas, P., Barton, E.D., 2002. Mesoscale patterns in the Cape São Vicente (Iberian Peninsula) upwelling region. *J. Geophys. Res.: Oceans* 107 (C10). <https://doi.org/10.1029/2000JC000456>, 28–1.
- Sánchez, R.F., Relvas, P., 2003. Spring–summer climatological circulation in the upper layer in the region of Cape St. Vincent, Southwest Portugal. *ICES J. Mar. Sci.* 60, 1232–1250. [https://doi.org/10.1016/S1054-3139\(03\)00137-1](https://doi.org/10.1016/S1054-3139(03)00137-1).
- Silva, A., Palma, S., Oliveira, P.B., Moita, M.T., 2009. Composition and interannual variability of phytoplankton in a coastal upwelling region (Lisbon Bay, Portugal). *J. Sea Res.* 62 (4), 238–249. <https://doi.org/10.1016/J.SEARES.2009.05.001>.
- Sousa, M.C., deCastro, M., Alvarez, I., Gomez-Gesteira, M., Dias, J.M., 2017. Why coastal upwelling is expected to increase along the western Iberian Peninsula over the next century? *Sci. Total Environ.* 592, 243–251. <https://doi.org/10.1016/J.SCITOTENV.2017.03.046>.
- Strohmeier, T., Strand, Ø., Alunno-Bruscia, M., Duinker, A., Cranford, P.J., 2012. Variability in particle retention efficiency by the mussel *Mytilus edulis*. *J. Exp. Mar. Biol. Ecol.* 412, 96–102. <https://doi.org/10.1016/j.jembe.2011.11.006>.
- Suplicy, F.M., 2020. A review of the multiple benefits of mussel farming. *Rev. Aquacult.* 12 (1), 204–223. <https://doi.org/10.1111/RAQ.12313>.
- Thorel, M., Fauchot, J., Morelle, J., Raimbault, V., Le Roy, B., Miossec, C., Kientz-Bouchart, V., Clauquin, P., 2014. Interactive effects of irradiance and temperature on growth and domoic acid production of the toxic diatom *Pseudo-nitzschia australis* (Bacillariophyceae). *Harmful Algae* 39, 232–241. <https://doi.org/10.1016/J.HAL.2014.07.010>.
- Trainer, V.L., Bates, S.S., Lundholm, N., Thessen, A.E., Cochlan, W.P., Adams, N.G., Trick, C.G., 2011. *Pseudo-nitzschia* physiological ecology, phylogeny, toxicity, monitoring and impacts on ecosystem health. <https://doi.org/10.1016/j.hal.2011.10.025>.
- Trainer, V.L., Pitcher, G.C., Reguera, B., Smayda, T.J., 2010. The distribution and impacts of harmful algal bloom species in eastern boundary upwelling systems. *Prog. Oceanogr.* 85 (1–2), 33–52. <https://doi.org/10.1016/J.POCEAN.2010.02.003>.
- Utermöhl, H., 1958. Zur Ver vollkommung der quantitativen phytoplankton-methodik. *Mitteilung Internationale Vereinigung Fuer Theoretische und Angewandte Limnologie* 9, 39.
- Vale, P., 2022. Cycles of marine biotoxins in bivalves and their spatial distribution along the continental Portuguese coast: are trends related to global change already discernible? *Reg. Environ. Change* 22 (4), 116. <https://doi.org/10.1007/s10113-022-01972-6>.
- Vale, P., Botelho, M.J., Rodrigues, S.M., Gomes, S.S., Sampayo, M.A. de M., 2008. Two decades of marine biotoxin monitoring in bivalves from Portugal (1986–2006): a review of exposure assessment. *Harmful Algae* 7 (1), 11–25. <https://doi.org/10.1016/J.HAL.2007.05.002>.
- Vale, P., Sampayo, M.A.M., 2001. Domoic acid in Portuguese shellfish and fish. *Toxicol.* 39 (6), 893–904. [https://doi.org/10.1016/S0041-0101\(00\)00229-4](https://doi.org/10.1016/S0041-0101(00)00229-4).
- Van Houcke, J., Medina, I., Maehre, H.K., Cornet, J., Cardinal, M., Linssen, J., Luten, J., 2017. The effect of algae diets (*Skeletonema costatum* and *Rhodomonas baltica*) on the biochemical composition and sensory characteristics of Pacific cupped oysters (*Crassostrea gigas*) during land-based refinement. *Food Res. Int.* 100, 151–160. <https://doi.org/10.1016/J.FOODRES.2017.06.041>.
- WoRMS. Editorial Board, 2024. World register of marine species. Available from: <https://www.marinespecies.org/VLIZ> (Accessed 19 October 2024). <https://doi.org/10.14284/170>.